

**ADDIS ABABA UNIVERSITY**  
**SCHOOL OF GRADUATE STUDIES**  
**DEPARTMENT OF CHEMISTRY**



**GRADUATE PROJECT (Chem. 774)**

**ELECTROCHEMICAL DETERMINATION OF CATECHOL  
USING MODIFIED ELECTRODE**

**By**

**TIZITA G/HIWOT**

**ADVISOR:**

**MERID TESSEMA (Ph.D)**

June 2014

**ADDIS ABABA UNIVERSITY**  
**SCHOOL OF GRADUATE STUDIES**  
**DEPARTMENT OF CHEMISTRY**  
**GRADUATE PROJECT (Chem. 774)**

**ELECTROCHEMICAL DETERMINATION OF CATECHOL  
USING MODIFIED ELECTRODE**

By

Tizita G/Hiwot

June 2014

Approved by the examining board

Signature

date

Dr. Merid Tessema

\_\_\_\_\_

\_\_\_\_\_

(Advisor)

Prof. Tewodros Solomon

\_\_\_\_\_

\_\_\_\_\_

(Examiner)

Dr. Solomon Mehretie

\_\_\_\_\_

\_\_\_\_\_

(Examiner)

## **Acknowledgments**

I am grateful to Dr. Merid Tessema for all his guidance, motivation and support during this work.

I would also like to gratefully thank Ato Negussie Negash for all the helpful support, collaboration, and discussion and for giving technical aid and assistance in every day laboratory problems.

My thanks are also extended to Ato Mola Tefera for helpful discussions; to all my friends for making my time enjoyable at Addis Ababa University.

I would like to thank Addis Ababa University Msc Scholarship for the financial support and the Department of Chemistry for allowing to join the Post Graduate Program.

Finally I would like to thank my parents for all their love and support.

## Table of Contents

Acknowledgments.....	i
List of Figures .....	iv
List of Tables .....	vi
List of Abbreviations .....	vi
1. Introduction.....	1
1.1. General properties of catechol.....	1
1.1.1 .Natural occurrence of catechol .....	1
1.1.2. Physical Properties of catechol.....	2
1.1.3. Chemical Properties of Catechol .....	2
1.1.4. Redox chemistry.....	3
1.1.5. Uses and applications .....	4
1.1.6. Metabolism of catechol .....	4
1.1.7. Health and Environmental effects of Catechol.....	4
1.1.7.1. Health effects.....	4
1.1.7.2. Environmental effects.....	5
1.1.8. Synthesis of catechol .....	5
1.2. Conducting polymers .....	6
1.2.1. Poly (3, 4-ethylenedioxythiophene) (PEDOT).....	7
1.2.2. Synthesis of PEDOT.....	8
1.2.3. Applications of PEDOT.....	9
1.3. Carbon Nanotubes .....	10
1.3.1. Single-walled Carbon Nanotube.....	11
1.3.2. Multi-walled Carbon Nanotubes .....	11
1.4. Electrodes .....	12
1.4.1. Working Electrode.....	12
1.4.1.1 glassy carbon electrode.....	13
1.4.2. Reference Electrode.....	13
1.4.3. Counter Electrode .....	14
1.5. Electroanalytical Techniques .....	14

1.5.1. Cyclic voltammetry .....	15
1.5.2. Reversible System .....	18
1.5.3. Differential pulse voltammetry.....	19
1.5.4 Method of catechol detection .....	21
2. Objective of the study .....	22
2.1. General Objective.....	22
2.2. Specific objective .....	22
3. Experimental part.....	23
3.1. Reagents and chemicals .....	23
3.2. Instruments and Apparatus.....	23
3.3. Electrode Characterization .....	23
3.3.1. Electrochemical cell and electrode .....	23
3.3.2. Preparation of the glassy carbon electrode .....	24
3.3.3. Modification of the glassy carbon electrode.....	24
3.3.4. Modification of PEDOT /GC electrode by SWCNT .....	25
3.3.5. Cyclic voltammetric investigation.....	27
4. Results and discussion .....	27
4.1. Effect of scan rate.....	28
4.2. Effect of ionic strength.....	32
4.3. Effect of the pH of the supporting electrolyte.....	33
4.4. Differential pulse voltammetric investigation.....	35
4.4.1 Effect of pulse amplitude.....	36
4.4.2. Effect of pulse width.....	336
4.4.3. Effect of pulse period .....	37
4.4.5. Optimized Experimental Conditions .....	38
4.5. Linear Range and Detection Limit .....	38
4.6. Effect of Interferences .....	41
4.7. Simultaneous determination of hydroquinone and catechol .....	44
4.8 Analytical applications .....	48
4.8.1 Analysis of Catechol in tap water.....	48

4.8.2. Analysis of catechol in tea samples.....	49
5. Conclusion .....	51
6. References.....	52

## List of Figures

<b>Figure 1.</b> The structure of the three isomers.....	1
<b>Figure 2.</b> Chemical reactions of catechol in the environment.....	3
<b>Figure 3.</b> Oxidation of catechol.....	3
<b>Figure 4.</b> Chemical structure of EDOT.....	8
<b>Figure 5.</b> demonstration of the molecular structure of PEDOT.....	8
<b>Figure 6.</b> Single-walled carbon nanotubes .....	11
<b>Figure 7.</b> Multi-walled carbon nanotubes .....	12
<b>Figure 8.</b> Working electrodes .....	12
<b>Figure 9.</b> A typical silver-silver chloride reference electrode.....	14
<b>Figure 10.</b> Counter electrodes. ....	14
<b>Figure 11.</b> A cyclic voltammetry potential waveform with switching potentials.....	16
<b>Figure 12.</b> The expected response of a reversible redox couple during a single potential cycle..	16
<b>Figure 13.</b> Excitation waveform of the differential pulse voltammetry.....	21
<b>Figure 14.</b> Typical set up of an instrument for voltammetric measurements.....	24
<b>Figure 15.</b> Cyclic voltammograms for the electropolymerisation of PEDOT film on the glassy carbon electrode in 0.01 EDOT solutions.....	25
<b>Figure 16.</b> Voltammograms of 100 $\mu$ M catechol at different electrodes (a)bare GCE,(b)SWCNTs/GCE, (c) PEDOT/GCE and (d) SWCNTs/PEDOT/GCE at a scan rate of 100 mVs <sup>-1</sup> in 0.2 M PBS solution (pH 7.0). ....	26
<b>Figure 17.</b> Cyclic voltammograms of 100 $\mu$ M catechol in 0.2 M KH <sub>2</sub> PO <sub>4</sub> -K <sub>2</sub> HPO <sub>4</sub> Buffer (pH = 7) at GCE with scan rate of 100 mV /s. ....	27

<b>Figure 18.</b> Cyclic voltammograms recorded at SWCNTs/PEDOT/GCE for 100 $\mu\text{M}$ catechol in 0.20 M ( $\text{KH}_2\text{PO}_4$ - $\text{K}_2\text{HPO}_4$ ) (pH 7.0) at different scan rates: a–n:0.02,0.05, 0.08, 0.10, 0.13,0.15,0.18,0.20, 0.25, 0.30, 0.35, 0.40, 0.45 and 0.5 V/s. ....	28
<b>Figure 19.</b> The dependence of the peak current on square root of scan rate. ....	29
<b>Figure 20.</b> The dependence of the peak potential $E_p$ on $\log v$ . ....	30
<b>Figure 21.</b> Effect of the pH on DPV response of the modified GC electrode for 100 $\mu\text{M}$ catechol; 0.2 M in phosphate buffer solution.....	33
<b>Figure 22.</b> Plot of DPV anodic peak current as a function of pH for 100 $\mu\text{M}$ , catechol. ....	34
<b>Figure 23.</b> Plot of DPV anodic peak potential as a function of pH for 100 $\mu\text{M}$ catechol.....	35
<b>Figure 24.</b> Oxidation of catechol.....	35
<b>Figure 25.</b> Plot of anodic peak current as a function of differential pulse amplitude.....	36
<b>Figure 26.</b> Plot of anodic peak current as a function of differential pulse width.....	37
<b>Figure 27.</b> Plot of anodic peak current as a function of differential pulse period.....	37
<b>Figure 28.</b> Differential pulse voltammograms for SWCNTs/PEDOT/GC modified electrode for different concentrations of catechol. Pulse amplitude 100 mV, pulse width 50 ms and pulse period 300 mV. ....	39
<b>Figure 29.</b> Plot of DPV anodic peak current as a function of catechol concentration from 6 to 100 $\mu\text{M}$ .....	41
<b>Figure 30.</b> Differential pulse voltammograms for SWCNTs/PEDOT/GC modified electrode for (a) 40, (b) 100, (c) 200 and (d) 2000 $\mu\text{M}$ ascorbic acid. Amplitude 100 mV, pulse width 50 ms and pulse period 300 mV.....	42
<b>Figure 31.</b> Differential pulse voltammograms at SWCNTs/PEDOT/GC modified electrode for (a) 0, (b) 20, (c) 40, (d) 100,(e) 200 and (f) 2000 $\mu\text{M}$ hydroquinone, Amplitude 100 mV, pulse width 50 ms and pulse period 300 mV.....	43
<b>Figure 32.</b> Differential pulse voltammograms for SWCNTs/PEDOT/GC modified electrode for (a) 0, (b) 20, (c) 40, (d) 100,(e) 200 and (f) 2000 $\mu\text{M}$ uric acid, Amplitude 100 mV, pulse width 50 ms and pulse period 300 mV. ....	44
<b>Figure 33.</b> DPVs for the binary mixtures of hydroquinone and catechol at SWCNTs/PEDOT/GC modified electrode in 0.2 M PBS (pH 7), [catechol] was kept constant and [hydroquinone] was changed (i.e., [catechol] = 2 $\mu\text{M}$ , [catechol]: (a) 20, (b) 40, (c) 60, (d) 70, (e) 80, (f) 100, (g) 150 $\mu\text{M}$ .....	45
<b>Figure 34.</b> Calibration plot of hydroquinone in the presence of 20 $\mu\text{M}$ catechol.....	46

**Figure 35.** DPVs for the binary mixtures of hydroquinone and catechol at SWCNTs/PEDOT/GC modified electrode in 0.2 M PBS (pH 7), [hydroquinone] was kept constant and [catechol] was changed (i.e., [hydroquinone] = 20  $\mu$ M, [catechol]: (a) 20, (b) 40, (c) 60, (d) 70, (e) 80, (f) 100, (g) 150  $\mu$ M)..... 47

**Figure 36.** Calibration plot of catechol in the presence of 20  $\mu$ M hydroquinone..... 48

## List of Tables

Table 1. Names, structures, and doping material of some common conducting polymers.....7

Table 2. The dependence of the peak current on the square root of the scan rate.....31

Table 3. The dependence of peak potentials on the logarithm of scan rate..... 32

Table 4. Optimum experimental conditions for the determination of catechol by DPV as SWCNTs /PEDOT/GC modified electrode. .... 38

Table 5. Comparison of different modified electrodes for catechol determination ..... 40

Table 6. Recovery study for catechol in tap water samples..... 49

Table 7. Recovery study for catechol in tea samples..... 50

## List of Abbreviations

<b>CA</b>	Chronoamperometry
<b>CE</b>	Counter electrode
<b>CNT</b>	Carbon nanotube
<b>CME</b>	Chemically modified electrode
<b>CP</b>	Chronopotentiometry
<b>CPs</b>	Conducting polymers
<b>CV</b>	Cyclic voltammetry

<b>DPV</b>	Differential pulse voltammetry
<b>EDOT</b>	3, 4-Ethylene dioxthiophene
<b>E</b>	Potential
$\Delta E$	Change in potential
$E^{1/2}$	Half wave potential
$E_{pc}$	Cathodic peak potential
$E_{pa}$	Anodic peak potential
<b>GCE</b>	Glassy carbon electrode
<b>HQ</b>	Hydroquinone
<b>i</b>	Current
$i_{pa}$	Anodic peak current
$i_{pc}$	Cathodic peak current
<b>MWCNT</b>	Multi wall carbon nanotube
<b>M</b>	Molar
<b>NPV</b>	Normal pulse voltammetry
<b>n</b>	Number of electron
<b>PBS</b>	Phosphate buffer solution
<b>PANI</b>	Polyaniline
<b>PPY</b>	Polypyrroles
<b>PEDOT</b>	Poly (3, 4-Ethylene dioxthiophene)
<b>s</b>	Second
<b>SWCNT</b>	Single wall carbon nanotube
<b>TEM</b>	Transmission electron microscope
<b>RE</b>	Reference electrode

## **Abstract**

A simple, sensitive and selective electrochemical method for determination of catechol has been developed at a glassy carbon electrode modified with single walled carbon nanotubes (SWCNT) and poly (3, 4 ethylenedioxythiophene) (PEDOT) conducting polymer through the oxidation of catechol. The oxidation potential of catechol on the SWCNTs/PEDOT/GC modified electrode was much lower and the oxidation currents were higher compared to the bare electrode. Under the optimum conditions, the differential pulse voltammetric current of the sensor was linear in the concentration range 6 – 100  $\mu\text{M}$  with a detection limit of 0.18  $\mu\text{M}$ . The detection limit is comparable or better than many electrochemical methods currently reported for catechol determination, and the sensor is cheaper and easier for fabrication. The sensor was not only convenient for quantifying catechol in the presence of common interferences but also capable of detection in tea samples and tap water.

**Keywords:** Electrochemistry, conducting polymer, electropolymerisation, single wall carbon nanotube, poly (3, 4-ethylenedioxythiophene), modified, electrode, catechol

## 1. Introduction

### 1.1. General properties of catechol

Catechol (1, 2-benzenediol or 1, 2-dihydroxybenzene) is an important class of dihydroxybenzene compounds, which is an aromatic compound in which two hydroxyl groups are substituted onto a benzene ring; because it has at least one hydroxyl group covalently bonded directly to a carbon atom in a benzene ring. It belongs to a class of organic compounds called phenols [1]. It is isomeric with hydroquinone and resorcinol.

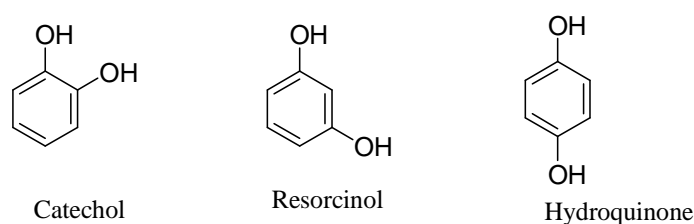


Figure 1. The structure of the three isomers

#### 1.1.1 .Natural occurrence of catechol

Catechol, also known as Pyrocatechol or 1, 2-dihydroxybenzene is an organic compound with the molecular formula  $C_6H_4(OH)_2$ . Catechol is the ortho isomer of the three isomeric benzenediols. This colourless compound occurs naturally in trace amounts. Catechol occurs as feathery white crystals which are very rapidly soluble in water. Catechol occurs naturally in trace amount in higher plants such as teas, vegetables, fruits, tobaccos and some traditional Chinese medicines [2]. Catechol has been identified in roasted coffee beans and in the leaves of blueberry, cranberry, cowberry and bearberry plants; in addition, tea is prepared from these leaves that have been reported to contain catechol at concentrations up to 1% of total ingredients [3]. The hazardous substances data bank (HSDB) in 1993 reported catechol is found in onions, apples, and even in the leaves or branches of oak and willow trees. Synthetic catechol is made by hydroxylation of phenol. It is only used in industry as an intermediate for chemical synthesis, mainly for aroma products, agrochemicals and pharmaceuticals or in formulation. The pure substance has antioxidant properties that may cause damage to human health. It is toxic by oral

and dermal routes and harmful by inhalation, causes skin irritation and serious eye damage, may cause an allergic skin reaction and is suspected of causing genetic defects. The pure substance is only used in industry and is handled under stringent safety conditions in accordance with the risk management measures to control the risk of exposure and preserve human health and environment.

### **1.1.2. Physical Properties of catechol**

1, 2-Benzenediol is colourless with a weak odour and unpleasant sweet taste of organic solid substance and become brown on exposure to air and light and pink on contact with air and light [4]. Also when it exposed to oxygen, such as an apple or pear is cut, the catechol turns dark. 1,2-Benzenediol has boiling point of 245 °C and a melting point of 105 °C, very soluble in colourless with a weak odour of water, benzene, chloroform, diethyl ether, ethanol, pyridine and aqueous alkalis [5,6] and its vapour pressure is 4 Pa at 20°C; relative vapour density (air = 1), 3.79 [7].

### **1.1.3. Chemical Properties of Catechol**

Catechol can undergo a variety of chemical reactions, such as complex formation and redox chemistry of catechol. In presence of heavy metals such as iron or copper, stable complexes can be formed. In the presence of oxidizing agents, catechol can be oxidized to semiquinone radicals and in the next step to o-benzoquinones. Heavy metals may catalyze redox reactions in which catechol are involved. As a consequence of the chemical properties and the chemical reactions of catechol, many different reactions can occur with biomolecules such as DNA, proteins and membranes, ultimately leading to non repairable damage. Reactions with nucleic acids such as adduct formation and strand breaks. Interactions with proteins causing protein and enzyme inactivation are also delineated [8]. The oxidation of catechol is a fairly reversible 2e- processes leading to the o-quinone. The interest in catechol centres on the high reactivity of this o-quinone and it has provided an excellent substrate for their measurement of rapid 1, 4-addition reaction. The first such reaction involved the important class of biogenic catecholamine, adrenaline, noradrenalin, also known as epinephrine and norepinephrine respectively, dopamine and related substances. Due to its biological importance and toxicity effects catechol needs rapid and sensitive methods to detect it.

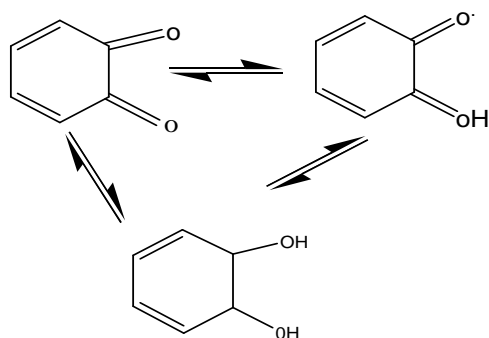


Figure 2. Chemical reactions of catechol in the environment

### 1.1.4. Redox chemistry

Catechol is a relatively non polar molecule which allows it to be easily taken up by the cell but not easily expelled. The unbalanced accumulation of any foreign species in the cell can lead to the destruction of the cell. Furthermore, upon oxidation catechol acts very similar formation of free radicals and it will bind to critical cell component such as lipids, protein and DNA. The binding destroys the functionality of the component in the cell. Catechol was deemed a federal hazardous pollutant in 1993 and studies have shown that it may even have carcinogenic effects on the cell. The oxidation of catechol the hydrogen atoms are pulled off and become an ortho benzoquinones or o-quinone for short. The o-quinone acts as an oxidizing agent and will reverse back to the original catechol structure after being reduced. The oxidation or reduction process can be either chemically or electrochemically stimulated this process shown below. The o-quinone is highly unstable and will readily bond to any nucleophilic surface. The toxicity to the cells results from this o-quinone binding to vital cell structure, but this readily binding nature can be taken advantage of to detect the concentration of the o-quinone as they bind to a particular surface [9].

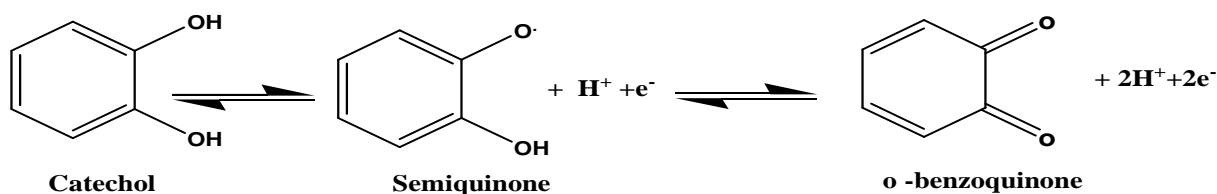


Figure 3. Oxidation of catechol

### **1.1.5. Uses and applications**

Catechol is used in a variety of applications. It is used as a reagent for photography, textile, paper, steel, petrochemical, rubber, dyeing fur, plastic, pesticides, wood preservatives, tanning lotion, cosmetic creams, petroleum refinery, pharmaceutical and in the wastewater of synthetic coal fuel conversion processes. The effluents from synthetic coal fuel conversion processes may contain catechol concentrations ranging from 1 to 1000 mg/l [8, 10] and as an intermediate for the synthesis of pharmaceuticals, agrochemicals and in formulation. In the pharmaceutical industry [11], substituted catechol, especially chlorinated and ethylated, catechols are by-products in pulp and oil mills [8]. Catechol is intermediary products from the degradation of aromatic compounds and lignin by microorganism. Also catechol is a precursor to various flavourings such as vanillin, used in food industry, perfumery, home and personal care products.

### **1.1.6. Metabolism of catechol**

Catechol can occur as metabolites in the degradation of benzene or estrogens [12] or as endogenous compounds, such as neurotransmitter and their precursors such as adrenaline, noradrenalin, dopamine and L-DOPA (L-3, 4-dihydroxy-phenylalanine). Additionally, catechol can be taken up in the form of tobacco smoke as catechol, semiquinone and polymerized catechol or as food components for example catechol, dopamine, caffeic acid, tea catechin. In 1950, it was suggested that benzene metabolites were responsible for the benzene toxicity in mammals and humans.

### **1.1.7. Health and Environmental effects of Catechol**

#### **1.1.7.1. Health effects**

The International Agency for Research on Cancer (IARC 1999) has classified 1,2-benzenediol as “possibly carcinogenic to humans” based on sufficient evidence of carcinogenicity in 1000000 experimental animals. It has been reported that long-term administration of 1,2-benzenediol in the diet induces adenocarcinoma of the glandular stomach in several strains of rats (IARC 1999); however, it caused gene mutations, chromosomal aberrations and sister chromatid exchanges in mammalian cells. 1,2-Benzenediol induced DNA strand breaks, gene mutations, chromosomal

aberrations, an euploidy and cell transformation in non-human mammalian cells with or without metabolic activation. Additionally, catechol act both as antioxidant, preventing lipid peroxidation, and as pro-oxidant damaging macromolecules such as DNA and proteins. Catechol can also destroy membrane functioning due to their redox cycling activity on the other hand, catechol is readily absorbed from the gastrointestinal tract, renal tube degeneration, liver function decrease, cancers, and neurodegenerative diseases, besides accumulating in bone marrow [13] also effects on dermal and oral routes of exposure and harmful if inhaled, causes skin irritation, skin sensitizer, depressant of the central nervous system. Catechol also causes eye burns that are slow to heal and serious eye damage, may cause an allergic skin reaction and is suspected of causing genetic defects.

#### **1.1.7.2. Environmental effects**

Based on its physical and chemical properties, catechol was released in the environment, it would be mainly distributed in the water [14]. Catechol being very soluble, it is not susceptible to deposit onto sediments. In addition, catechol is readily biodegradable, thus not persistent in the environment, and has a low potential for adsorption and bioaccumulation, so no significant distribution into soil and sediment compartments is expected. As a result, the exposure of sedimentary and terrestrial organisms is judged to be very low. All industrial aqueous releases that may contain the substance are directed to a waste water treatment plant. The potential of distribution in the atmosphere is very low and if catechol was released into the air, it would be readily photo degraded, so no significant air exposure is expected. Human risk of exposure via the environment is expected to be low since catechol is readily biodegradable and non bioaccumulative.

#### **1.1.8. Synthesis of catechol**

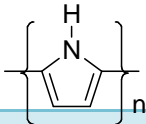
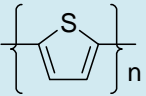
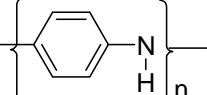
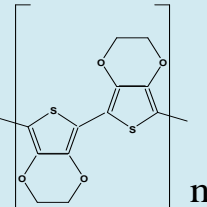
Catechol is formed by the heating of catechin above its decomposition point. catechol is produced industrially by the hydroxylation of phenol using hydrogen peroxide [15]. Catechol has also been produced by the hydrolysis of 2-substituted phenols, especially 2-chlorphenol, with hot aqueous solutions containing alkali metal hydroxides. Its methyl ether derivative, converts to catechol via hydrolysis of the  $\text{CH}_3\text{-O}$  bond as promoted by hydriodic acid. It may be prepared

synthetically by fusing 3-iodophenol, phenol-3-sulfonic acid or benzene-1,3-disulfonic acid with potassium carbonate; by the action of nitrous acid on 3-aminophenol, or by the action of 10% HCl on 1,3-diaminobenzene. Many ortho- and Para-compounds of the aromatic series (for example, the bromophenols, benzene-para-disulfonic acid) also yield by fusion with potassium hydroxide. Hydroquinone is obtained from few methods: oxidation of aniline with manganese dioxide and sulphuric acid, followed by reduction with iron dust and water. The second method consists of the alkylation of benzene with propylene to produce a mixture of diisopropyl benzene isomers from which, in a first step, the Para-isomer is isolated. This is oxidized with oxygen to produce the corresponding dihydroperoxide, which is treated with an acid to produce hydroquinone and acetone. Finally, the oxidation of Phenol with hydrogen peroxide can be used to produce a mixture of products from which both hydroquinone and catechol (1, 2-dihydroxybenzene) can be isolated.

## **1.2. Conducting polymers**

During the last few decades, conducting polymers have been gathering a great interest in academia and industry by providing the opportunity of combining the electrical properties of a semiconductor and metals with the traditional advantages of conventional polymers such as easy and low cost preparation and fabrication. After the discovery made by Alan Mac Diarmid and co-workers in 1971 that polyacetylene can gain the conductivity of a metal by doping with  $I_2$ ,  $Br_2$  or  $AsF_5$ , many aromatic conjugated polymers were studied. Now a days, most of the researches about conducting polymers are focused on Polyaniline (PANI), Polypyrroles (PPY), Polythiophene (PTh) and Poly (3, 4 ethylenedioxythiophene) (PEDOT) as they possess relatively high conductivities and exhibit reasonable air stabilities [15]. The conductivity of such polymers is the result of several processes [16].

Table 1. Names, structures, and doping material of some common conducting polymers

polymers	structure	Doping material
polyacetylene	$(\text{CH})_n$	$\text{I}_2, \text{Br}_2, \text{Li}, \text{Na}, \text{AsF}_5$
Poly pyrrole		$\text{BF}_4^-, \text{ClO}_4^-$
Poly thiophene		$\text{BF}_4^-, \text{ClO}_4^-$
polyaniline		$\text{BF}_4^-, \text{ClO}_4^-$
Poly(3,4-ethylenedioxythiophene)		

### 1.2.1. Poly (3, 4-ethylenedioxythiophene) (PEDOT)

In the 1980s, scientist at Bayer AG research in Germany developed a new PTh derivative called poly (3, 4-ethylenedioxythiophene) (PEDOT) and known under the trade name Baytron. Indeed, Heywang and Jonas 1992 were the first to report the electrochemical synthesis of PEDOT. The monomer of PEDOT, called 3, 4-ethylenedioxythiophene (EDOT) presented some specific physical and chemical properties. EDOT has a boiling point of 225 °C and it will slowly turn to dark upon exposure to air and light because of partial oxidation. Substitution of the H on position 3 and 4 of thiophene by an O-electron donor (Figure 4) significantly lowers the oxidation of EDOT compared to thiophene. These donating groups also stabilise the positive charge generated in doped PEDOT [17].

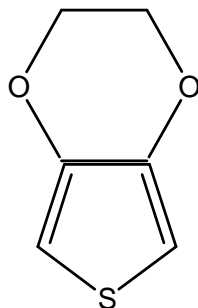


Figure 4. Chemical structure of EDOT

Due to these intrinsic features, PEDOT has become one of the most popular conducting polymers being studied by many scientific research groups. Among a number of conjugated polymers (conducting polymers), PEDOT has shown some advantages. PEDOT shows better properties such as high conductivity, environmental stability and high transparency [18] low oxidation potential, relatively low band gap, good chemical and electrochemical properties. However, EDOT and PEDOT have a drawback of being water insoluble/partially soluble both in neutral forms.

### 1.2.2. Synthesis of PEDOT

PEDOT and its derivatives can be synthesised in three ways i.e. oxidative chemical polymerization, electrochemical polymerization and transition metal-mediated coupling of derivatives of EDOT. There are different electrochemical techniques. For the electrochemical oxidation and polymerization of PEDOT such as cyclic voltammetry, chronoamperometry and chronopotentiometry were used to synthesise PEDOT and copolymer based EDOT [19]. By using these electroanalytical techniques, only short time of polymerization is needed and only a small amount of monomer is required.

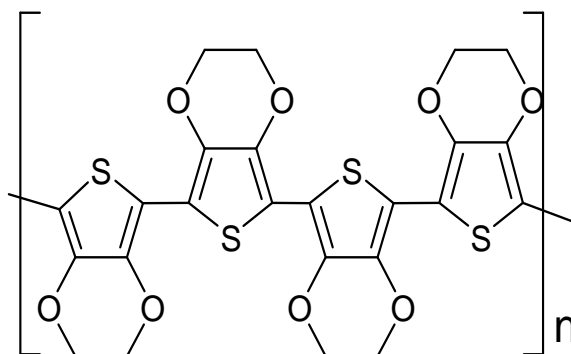


Figure 5. Demonstration of the molecular structure of PEDOT

### 1.2.3. Applications of PEDOT

CPs are electro active materials, thus the properties depend on the degree of oxidation (p-doping) and reduction (n-doping) of the conjugated back bone[20]. In the undoped state, CPs is organic semiconductors with a suitable band gap to transform electricity into light and vice versa. These features make the CP suitable for solar cells and hole injection layer in light emitting diodes based organic materials (OLED). Among the CPs, polypyrroles and polyaniline can be easily synthesised by chemical and electrochemical polymerizations but the poor stability of these polymers is an obstacle for potential applications. On the other hand, polythiophene is a relatively stable conducting polymer but the synthesis by electrochemical method is very tricky because of the high oxidation potential of thiophene (+1.60 V vs SCE). This problem has been overcome by the discovery of new monomer, EDOT. Due to the salient features exhibited by PEDOT, it can be used in the field of anti-static coating, electrochromic devices as a matrix to entrap the enzyme solid state capacitors, electroluminescent devices, and as under layers for metallization of printed circuit boards. CP can also be used to fabricate low cost all-polymer transistor circuits by high-resolution inkjet printing [21]. CPs can be also synthesised in aqueous solutions. Avoiding the use of non-aqueous solvents renders the conjugated polymers biocompatible and therefore, CPs produced can be extensively used in the fabrication of inexpensive devices for development of biocompatible electrochemical sensors and biosensors in the medical diagnostic laboratories. Chemical sensors are miniaturized analytical. Poly (3, 4-ethylene dioxythiophene)(PEDOT) presence of specific compounds or ions in samples. In chemical sensor, initially, ion recognition process takes place followed by the conversion of the

chemical signal into an electrical signal by transducer. The properties of CP can be tailored for specific application by incorporation of a various types of dopants (counter ions) from relatively small to bulky biological molecules into the conducting polymer during electrochemical polymerization. One of the possible applications using this approach is the fabrication of chiral electrodes. PEDOT deposited on electrode becomes chiral PEDOT by doping with chiral dopants and can be used as chiral selectors [22].

### **1.3. Carbon Nanotubes**

In 1991, the Japanese electron microscopist, Sumio Iijima (a researcher at the NEC laboratory in Tsukuba, Japan) discovered that carbon could be made to a form of tubular structures while he was studying the material deposited on the cathode during the arc-evaporation synthesis of fullerenes [23]. By using transmission electron microscope (TEM) to magnify carbon ash, he found that the cathode deposit contained a variety of closed graphitic structure. In that ash he found tiny cylinders made of carbon atoms with the diameters in the order of nanometres and he called the cylinders nanotubes. The graphite layer appears somewhat like "a rolled-up chicken wire" with a continuous unbroken hexagonal mesh and carbon at the apexes of the hexagons. Therefore, it was found that when an electric arc struck between two carbon electrodes in inert gas atmosphere carbon nanotubes are synthesized. Therefore, it can be thought that the newly discovered carbon variety as an elongated fullerene type and spherical fullerenes are sometimes called buck balls, while cylindrical fullerenes are called buck tubes or nanotubes [23, 24, and 25]. Carbon nanotubes are a tube-shaped materials made up of carbon that has a diameter of measuring on the nanometer scale. Their name derives from their size; nanotubes are on the order of only a few nanometers wide (on the order of one ten-thousandth the width of a human hair), and their length can be millions of times greater than their width. They can also be thought as of narrow sheets of a million or more carbon atoms linked together in a hexagonal rings connected as in graphite, but rolled in to a very long cylinder that is 1-2 nm in diameter. Internally by comparison, a hair is about 100,000 nanometers across. To illustrate how narrow the nanotubes are, a carbon nanotube long enough to reach from earth to the moon could be rolled into a ball of the size of poppy seed [26]. CNTs are unique tubular structures of nanometer diameter and have large length/diameter ratio. CNTs are divided into two main groups: single-walled carbon nano-tube (SWNT) and multi-walled carbon nanotubes (MWNT). SWNT can be

considered as a long wrapped graphene sheet by rolling it in certain directions. The properties of the nanotubes are mainly dictated by the rolling direction as well as the diameter. To sum up carbon nanotubes classified in to two that are SWNT and MWNT, which have different structure.

### 1.3.1. Single-walled Carbon Nanotube

The structure of a SWNT can be conceptualized by wrapping a one-atom-thick layer of graphite (graphene) into a seamless cylinder. The molecular structure of a carbon nanotube is often depicted as rolled chicken wire. Carbon nanotubes exist as a macromolecule of carbon analogous to a sheet of graphite rolled in to a cylinder [26]. SWCNT consists of two separate regions (the side wall and the end cap) with very different physical and chemical properties. The end-cap structure is similar to or derived from a small fullerene in which the carbon atoms are in both pentagon and hexagon rings. The side wall only consists of hexagon rings.

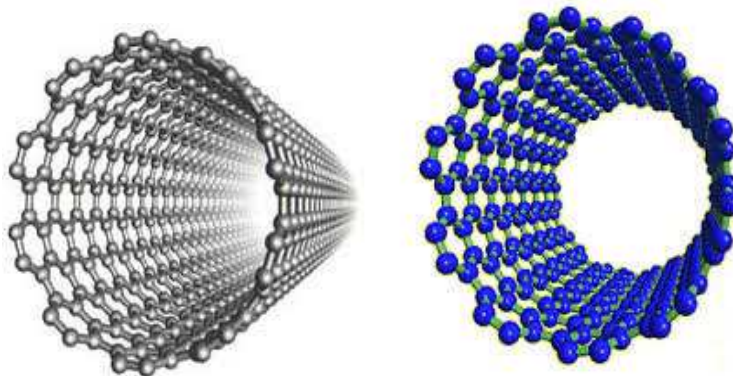


Figure 6. Single-walled carbon nanotubes

### 1.3.2. Multi-walled Carbon Nanotubes

Multi-walled carbon nanotubes are concentric cylindrical graphitic tubes [27]. They contain atomic layer planes of carbon, which form a nested series of concentric cylinders, much like the growth rings of on a tree. MWNTs have several characteristics: wall thickness, number of concentric cylinders, cylinder radius, and cylinder length [28]. Multi-walled nanotubes are invariably produced with a high frequency of structural defects that they frequently contain regions of structural imperfection and the occurrence of defects that inevitably degrade the material properties of a substance, such as strength.

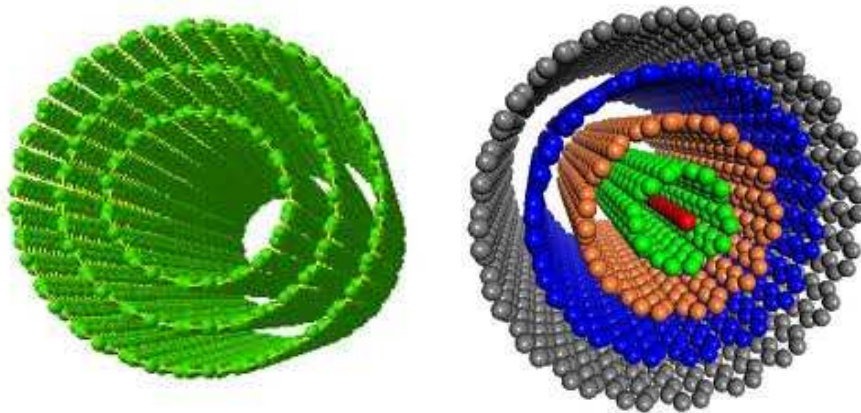


Figure 7. Multi-walled carbon nanotubes

## 1.4. Electrodes

Commonly there are three electrodes commonly used in electrochemistry experiments i.e. working electrode (WE), reference electrode (RE) and counter electrode (CE). Every electrode plays a vital role and brief explanations are given below.

### 1.4.1. Working Electrode

The working electrode (WE), consisting of inert conductors such as gold, platinum, carbon or mercury, is an electrode of interest on which electrochemical processes are studied. The analytical process of oxidation and reduction occurs at this electrode. The surface area of this electrode is typically just a few mm to limit the current flow.



Figure 8. Glassy Carbon Working electrodes

### **1.4.1.1. Glassy Carbon Electrode**

Glassy carbon has been very popular because of its excellent mechanical and electrical properties, wide potential window, chemical inertness (solvent resistance) and relatively reproducible performance. The structure of glassy carbon involves thin, tangled ribbons of cross-linked graphite-like sheets. Because of its high density and small pore size, no impregnating procedure is required. However surface treatment is usually employed to create active and reproducible glassy carbon electrodes and to enhance their analytical performance such pre-treatment is usually achieved by polishing (to the “mirror-like “appearance) with successively smaller alumina particles (down to 0.05  $\mu\text{m}$ ). The electrode should then be rinsed with deionized water before use. Additional activation steps, such as electrochemical, chemical, heat or laser treatments, have also been used to enhance the performance.

### **1.4.2. Reference Electrode**

A reference electrode (RE) is an electrode for which the electrode potential is known and constant. This electrode potential has to be stable (with time and temperature) and independent of the properties of the solution because it is used to measure/control the potential of the working electrode by the application of a voltage between them. This means that the electrode must be unaffected by the passage of the small amounts of current required in making potentiometric measurements. The high stability of the electrode potential is usually reached by employing a redox system with constant (Buffered or saturated) concentrations of each of the participants of the redox reaction. There are three common reference electrodes used i.e. saturated hydrogen electrode, silver-silver chloride (Ag/AgCl) and saturated calomel electrode (SCE). Figure 9 shows the relative potentials of the different reference electrodes used. Ag/AgCl electrode functions as a redox electrode and the reaction is between the silver metal (Ag) and its salt, silver chloride (AgCl). The Nernst equation shows the dependence of the potential of the Ag/AgCl electrode on the activity of chloride ions.

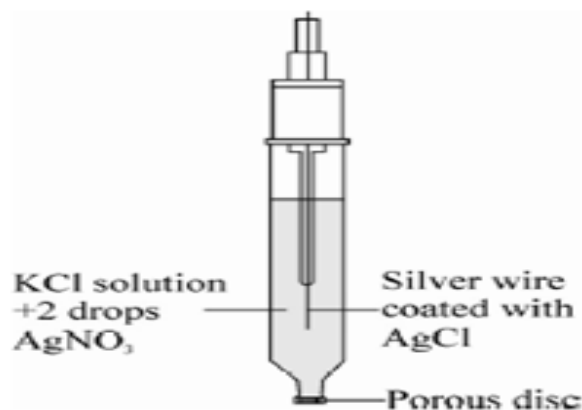


Figure 9. A typical silver-silver chloride reference electrode

### 1.4.3. Counter Electrode

The counter electrode (CE) is also known as the auxiliary electrode. It is used to complete the circuit (Figure 10) carrying the current flowing through the cell. The CE is of opposite polarity to the WE and typically has a larger surface area than the WE to ensure that the rate of redox reaction at the WE determines the current. The commonly used counter electrodes are platinum plate, platinum coil and a short length of platinum wire.



Figure 10. Counter electrodes

## 1.5. Electroanalytical Techniques

An electroanalytical technique encompasses a group of quantitative analytical methods that are based upon the electrical properties of a solution of the analyte when it is made a part of an electrochemical cell. These techniques are capable of producing exceptionally low detection limits and wealth of characterization information describing electrochemical addressable systems [29]. Electrochemical techniques are powerful and versatile analytical techniques that offer high

sensitivity, accuracy and precision as well as a large linear dynamic range. Electroanalytical measurements offer a number of important benefits: such as specificity, selectivity resulting from the choice of electrode material, high sensitivity and low detection limit, possibility of furnishing results in real time or close to real time and application as miniaturized sensors where other sensors may not be useful. Electrochemical measurements are two-dimensional, with the potential being related to qualitative properties (with thermodynamic or kinetic control) and the current related to quantitative properties (controlled either by mass transport process or reaction rates). Thus, compounds can be selectively detected by electrochemical methods. The principal criterion for electroanalytical measurements is that the species, which is desired to be measured, should react directly (or indirectly through coupled reaction) at or be adsorbed onto the electrode. Electroanalytical measurements can only be carried out in situations in which the medium between the two electrodes making up the electrical circuit is sufficiently conducting [29].

#### Advantages of Electroanalytical techniques

- ❖ Electroanalytical methods are well established and use relatively inexpensive equipment to produce unique characterization information for molecules and chemical systems: qualitative and quantitative analytical data, thermodynamic data and kinetic data.
- ❖ Electroanalytical methods are sensitive; they are able to detect sub micro molar concentrations and subpicomolar amounts of electro active material.
- ❖ Electroanalytical methods are selective; they are able to control the potential of an electrode, which makes it possible to determine the electrochemical “spectrum” of electro active species in solution, analogous to probing the energy states of a molecule with light via spectroscopy.

#### **1.5.1. Cyclic voltammetry**

Cyclic voltammetry is a very versatile electrochemical technique which allows to probe the mechanics of redox and transport properties of a system in solution. This is accomplished with a three electrode arrangement where by the potential relative to some reference electrode is scanned at a working electrode while the resulting current flowing through a counter (or auxiliary) electrode is monitored in a quiescent solution. The technique is ideally suited for a

quick search of redox couples present in a system; once located, a couple may be characterized by more careful analysis of the cyclic voltammogram. More precisely, the controlling electronic is designed such that the potential between the reference and the working electrodes can be adjusted but the big impedance between these two components effectively forces any resulting current to flow through the auxiliary electrode. Usually the potential is scanned back and forth linearly with time between two extreme values the switching potentials using triangular potential waveform (see Figure 11). When the potential of the working electrode is more positive than that of a redox couple present in the solution, the corresponding species may be oxidized (*i.e.* electrons going from the solution to the electrode) and produce an anodic current. Similarly, on the return scan, as the working electrode potential becomes more negative than the reduction potential of a redox couple, reduction (*i.e.* electrons flowing away from the electrode) may occur to cause a cathodic current.

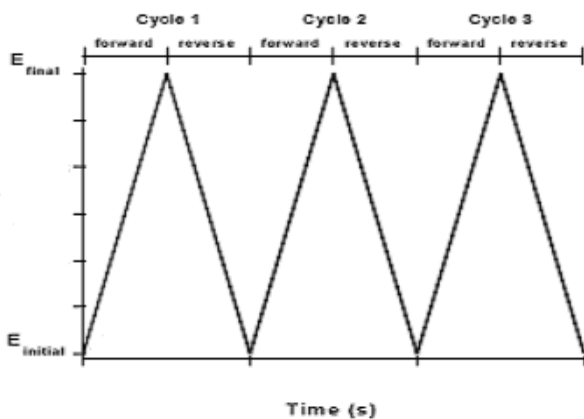


Figure 11. A cyclic voltammetry potential waveform with switching potentials

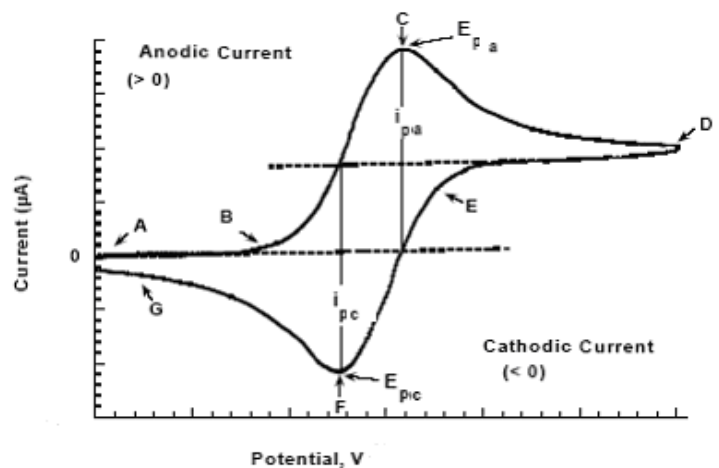


Figure 12. The response of a reversible redox couple during a single potential cycle.

By IUPAC convention, anodic currents are positive and cathodic currents negative [30]. The magnitude of the observed Faradaic current can provide information on the overall rate of the many processes occurring at the working electrode surface. As is the case for any multi-step process, the overall rate is determined by the slowest step. For an redox reaction induced at a working electrode, the rate determining step may be any one of the following individual step depending on the system: rate of mass transport of the electro-active species, rate of adsorption or de-sorption at the electrode surface, rate of the electron transfer between the electro-active

species and the electrode, or rates of the individual chemical reactions which are part of the overall reaction scheme.

For the oxidation reaction involving  $n$  electrons



The Nernst Equation gives the relationship between the potential and the concentrations of the oxidized and reduced form of the redox couple at equilibrium (at 298 K):

$$E = E^0 + \log_{10} \frac{[\text{Ox}]}{[\text{Red}]} \dots\dots\dots (1)$$

Where  $E$  is the applied potential and  $E^0$  the formal potential,  $[\text{ox}]$  and  $[\text{Red}]$  represent surface concentrations at the electrode/solution interface, not bulk solution concentrations. Note that the Nernst equation may or may not be obeyed depending on the system or on the experimental conditions. A typical voltammogram is shown in Figure. 12. The scan shown starts at a slightly negative potential, (A) up to some positive switching value, (D) at which the scan is reversed back to the starting potential. The current is first observed to peak at  $E_{pa}$  (with value  $i_{pa}$ ) indicating that an oxidation is taking place and then drops due to depletion of the reducing species from the diffusion layer. During the return scan the processes are reversed (reduction is now occurring) and a peak current is observed at  $E_{pc}$  (corresponding value,  $i_{pc}$ ). Providing that the charge–transfer reaction is reversible, that there is no surface interaction between the electrode and the reagents, and that the redox products are stable (at least in the time frame of the experiment), the ratio of the reverse and the forward current  $i_{pr}/i_{pf} = 1.0$  (in Figure 12  $i_{pa} = i_{pf}$  and  $i_{pc} = i_{pr}$ ). In addition, for such a system it can be shown that the corresponding peak potentials  $E_{pa}$  and  $E_{pc}$  are independent of scan rate and concentration, the formal potential for a reversible couple  $E^0$  is centered between  $E_{pa}$  and  $E_{pc}$ :  $E^0 = (E_{pa} + E_{pc})/2$  the separation between peaks is given by  $\Delta E_p = E_{pa} - E_{pc} = 59/n$  mV (for a  $n$  electron transfer reaction) at all scan rates (however, the measured value for a reversible process is generally higher due to uncompensated solution resistance and non-linear diffusion. Larger values of  $\Delta E_p$ , which increase with increasing scan rate, are characteristic of slow electron transfer kinetics). It is possible to relate the half-peak potential ( $E_{p/2}$ , where the current is half of the peak current) to the polar graphic

half-wave potential,  $E_{p/2} = E_{1/2} \pm 29\text{mV}/n$  (The sign is positive for a reduction process.) For multielectron-transfer (reversible) processes, the cyclic voltammogram consists of several distinct peaks, if the  $E^0$  values for the individual steps are successively higher and are well separated. An example of such mechanism is the six-step reduction of the fullerenes  $C_{60}$  and  $C_{70}$  to yield the hex anion products  $C_{60}^{6-}$  and  $C_{70}^{6-}$  where six successive reduction peaks can be observed.

### 1.5.2. Reversible System

A redox couple in which both species rapidly exchange electrons with working electrode is termed a reversible system. The redox reaction taking place in the solution can be expressed as:  $O + ne^- \leftrightarrow R$ , where O and R are the oxidized and reduced forms of the redox couple respectively. When the electron transfer rate in both the forward and reverse directions at the electrode is high, the process is described as reversible, and the cathodic and anodic peaks are separated by a potential of approximately  $59/n$  mV at  $25^\circ\text{C}$ , where n is the number of electrons transferred. If n electrons are transferred in a reaction that is reversible to distinguish between reversible (diffusion-controlled) and irreversible (charge-transfer controlled) kinetics of electrode process potential scan-rate is used as diagnostic tool – the rate of reagent transport is proportional to square root of scan-rate. Thus in one experimental set a shift in reversibility might be executed and analysis of  $\Delta E_p$  vs  $v^{1/2}$  gives information on reversibility and applicability of further calculations.. Reversible System Provided that the charge-transfer reaction is reversible, and that there is no surface interaction between the electrode and the reagents, and that the redox products are stable (at least in the time frame of the experiment) the ratio of the reverse and the forward current  $i_{pr}/i_{pf} = 1.0$ . Additionally, for such a system it can be shown that the corresponding peak potentials  $E_{pa}$  and  $E_{pc}$  are independent of scan rate and concentration.

$$\Delta E_p = E_{pa} - E_{pc} = 2.23 \frac{RT}{nF} = \frac{0.059}{n} \text{-----} \quad (2)$$

Where  $E_{pc}$  and  $E_{pa}$  are the potentials at which the oxidation and reduction processes occur, R is the universal gas constant, T is absolute temperature and F is Faraday's constant. Thus, the peak separation can be used to determine the number of electrons transferred, and as a criterion for a Nernstian behavior. Accordingly, a fast electron process exhibits  $\Delta E_p$  of about 59 mV. The

expression of the peak current for a reversible couple (at 25 °C) is given by the Randles-Sevcik equation:

$$i_p = (2.69 \times 10^5) n^{3/2} A C D^{1/2} v^{1/2} \text{ ----- (3)}$$

where,  $i_p$  is the peak current,  $n$  is the number of electron exchanged during the redox process,  $A$  is the active area of the working electrode,  $v$  is the scan rate,  $D$  and  $C$  are the diffusion coefficient and the bulk concentration of the electroactive species respectively. Accordingly, the peak current is directly proportional to the concentration and increases with the square root of scan rate. The relation of  $i_p$  to bulk concentration is particularly important in analytical applications and in studies of electrode mechanisms. The values of  $i_{pa}$  and  $i_{pc}$  are similar in magnitude for a simple reversible electron transfer reaction, i.e. their ratio is unity. However, the ratio of the peak current can be significantly influenced by the chemical coupled to the electrode process. For example, if there is a chemical reaction following the electron transfer reaction, the peak current on the reverse scan is decreased.

The position of the peaks on the potential axis ( $E_p$ ) is related to the formal potential of the redox

$$E^0 = \frac{E_{pc} + E_{pa}}{2} \text{ ----- (4)}$$

The diagnostic criterion of a single electron transfer reversible reaction is often sufficient to get qualitative as well as quantitative information about the thermodynamic and kinetic parameters of the system. The important quantities are peak potentials,  $E_{pa}$ ,  $E_{pc}$  and  $E_p/2$ , which provide a direct estimate of the electrode reversibility process. These indicate that for a given system the electrochemical equilibrium is always maintained at the electrode surface. The separation of peak potentials permits determination of  $E_{1/2}$  of the measured redox system [31].

### 1.5.3. Differential pulse voltammetry

This technique is similar to the normal pulse voltammetry in that the potential is also scanned with a series of pulses; however it differs from NPV because each potential pulse is fixed, of small amplitude (10 to 100 mV) and is superimposed on a slowly changing base potential. Current is measured at two points for each pulse, the first point just before the application of the pulse and the second at the end of the pulse [32]. These sampling points are selected to allow for

the decay of the non-faradic (charging) current. The difference between current measurements at these points for each pulse is determined and plotted against the base potential. For a reversible process the peak current is proportional to analyte concentration and it is given by:

$$i_p = \frac{nFAD^{1/2}C}{(\pi t_p)^{1/2}} (1 - \sigma)/(1 + \sigma) \text{-----(5)}$$

$$\sigma = \exp (NF\Delta E/2RT)$$

And the peak potential occurs at:

$$\Delta E_p = E_{1/2} - \Delta E_p/2 \text{----- (6)}$$

Where:  $t_p$  and  $\Delta E_p$  are pulse duration and amplitude of the voltage respectively. For small values  $\Delta E_p$ , the peak half width that is the width at  $i = i_p/2$  is 90.4 mV, but for larger pulse amplitude it Approaches the pulse amplitude. Differential pulse voltammetry has the following characteristics: Reversible reactions show symmetrical peaks and irreversible reactions show asymmetrical peaks, the peak potential is equal to  $E_{1/2} - \Delta E/2$  in reversible reactions, the peak current is proportional to the concentration and the detection limit is about  $10^{-8}$  M. The potential wave form consists of small pulses (of constant amplitude) superimposed upon a staircase wave form. The current is sampled twice in each pulse period (once before the pulse, and at the end of the pulse), and the difference between these two current values is recorded and displayed [33].

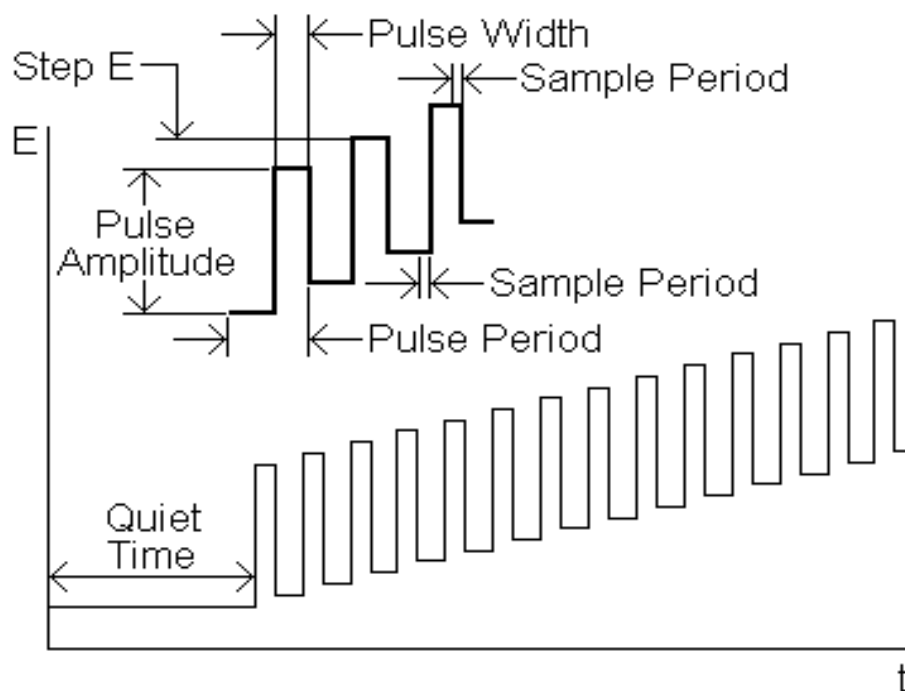


Figure 13. Excitation waveform of the differential pulse voltammetry

#### 1.5.4 Method of catechol detection

Until now, many analytical methods have been developed to determine catechol, such as Spectrophotometer, fluorescence, high performance liquid chromatography and chemiluminescence Gas chromatography, mass, spectrometer, electro chromatography and electrochemical methods. Among these methods, electrochemical methods have attracted more and more attention due to the advantages of fast response, cheap instrumentation, low cost, simple operation and time saving. However, for electrochemical methods, although many modified electrodes were developed for determination of catechol, the oxidation peaks of catechol could not be separated completely and would seriously overlap in cases of high concentrations. Some works have focused on the selective determination of catechol; however, selectivity still needs to be improved, especially in co-existence systems of hydroquinone, catechol and resorcinol [34].

## **2. Objective of the study**

### **2.1. General Objective**

To prepared SWCNT and PEDOT composite modified electrodes for the determination of catechol.

### **2.2. Specific objective**

- To examine the electrochemical behaviour and the electrocatalytic activity of SWCNTs and PEDOT using cyclic voltammetry and differential pulse voltammetry for the determination of catechol.
- To establish the optimum parameters for the sensitive determination of catechol i.e. to study the basic electroanalytical parameters required to determine catechol at the specified condition.
- To apply the electrodes prepared for the determination of catechol in real sample.

### **3. Experimental part**

#### **3.1. Reagents and chemicals**

All chemicals used were analytical grade and were used without any further purification: catechol (Indian industries), SWCNT (mixture of metallic and semiconducting) and 3, 4-ethylenedioxythiophene (EDOT) monomer were from Adrich, tetrabutylammonium perchlorate and acetonitrile were from Sigma-Aldrich potassium dihydrogen phosphate ( $\text{KH}_2\text{PO}_4$ ) and dipotassium hydrogen phosphate ( $\text{K}_2\text{HPO}_4$ ) (Fulka, Germany), alumina and doubly distilled water. Supporting electrolyte of phosphate buffer ( $\text{KH}_2\text{PO}_4$  -  $\text{K}_2\text{HPO}_4$ ) in the pH range 4-9 was prepared from 0.2 M  $\text{KH}_2\text{PO}_4$  and 0.2 M  $\text{K}_2\text{HPO}_4$  in distilled water. The pH of the solutions was adjusted by adding drops of concentrated  $\text{HNO}_3$  (Riedel-De Haen, Germany) and NaOH (Labmerk chemicals, India) by using a pH meter. Stock solution of catechol (1 mM) was prepared in 0.2 M phosphate buffer of pH 7.0. Experiments were carried out at the room temperature and all solutions were prepared from doubly distilled water was used throughout the work. The stock solution of catechol prepared was stored in the refrigerator to avoid exposure to air and light to keep its stability.

#### **3.2. Instruments and Apparatus**

The voltammetric experiments were performed using BAS-50 W potentiostat/galvanostat analyzer coupled with personal computer. A conventional three-electrode cell was used for measurements with a bare glassy carbon electrode (GCE) (3 mm diameter), SWCNT/PEDOT/GCE as the working electrode, Ag/AgCl (3 M KCl) as a reference electrode, and a platinum wire as counter electrode. An electronic digital balance was used to measure the weights of solid chemicals during solution preparation. The pH of the buffer solution was measured with a digital pH meter.

#### **3.3. Electrode Characterization**

##### **3.3.1. Electrochemical cell and electrode**

All the potentials are determined with respect to a saturated silver-silver chloride (calomel) electrode as the reference electrode and a platinum wire electrode as the counter electrode and a bare GCE or SWCNTs/PEDOT/GC modified electrode as the working electrode.



Figure. 14. Typical set up of an instrument for voltammetric measurements

### 3.3.2. Preparation of the glassy carbon electrode

The GCE surface is cleaned with high purity of 0.05  $\mu\text{M}$  alumina powder on a polishing cloth to obtain a mirror like, slurry electrode surface and washed with distilled water. The electrochemical pre-treatment has been done by using cyclic voltammetry with a potential scanning between -0.8 to + 0.8 V at 100 mV/s in 0.5 M  $\text{H}_2\text{SO}_4$  until a stable voltammograms was obtained. The cyclic voltammograms response was comparable with the electrochemical pre-treatment of GCE in pH 7.0 PBS. These processes were done before every experiment.

### 3.3.3. Modification of the glassy carbon electrode

The polymer film was deposited electrochemically from 0.01 mol/L of ethylenedioxythiophene (EDOT) monomer and 0.1 M tetra butyl ammonium per chlorate in acetonitrile. The polymer film was made by applying ten cycles in the range of -0.9 to + 1.5 V at scan rate of 100 mV/s. The film thickness was controlled by the number of cycles.

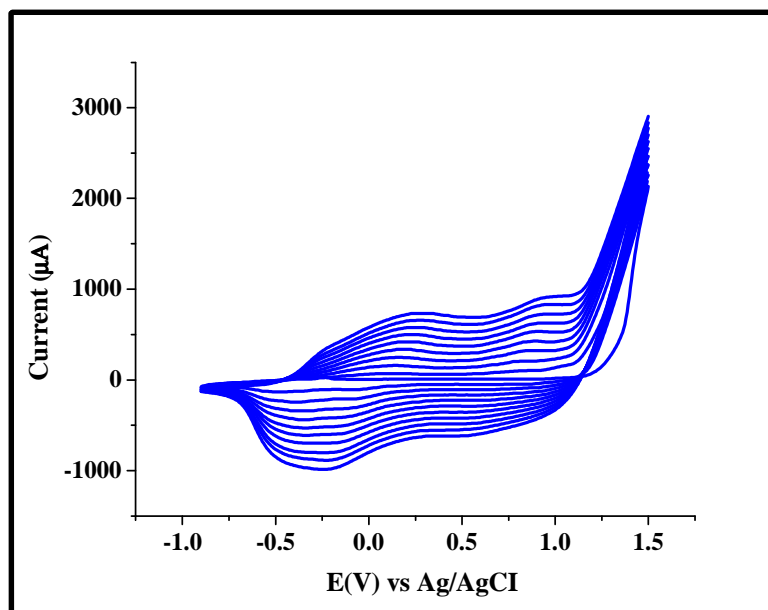


Figure 15. Cyclic voltammograms for the electropolymerisation of PEDOT film

### 3.3.4. Modification of PEDOT /GC electrode by SWCNT

The surface of the polymerized GC electrode was coated by 10 µL black suspensions of functionalized SWCNTs and the solvent was evaporated from the electrode surface at room temperature. Finally the modified electrode completely dried, it can be used 0.2 mol/L of phosphate solution at (pH = 7.0) with 100 µM of catechol was transferred into a cell and the three-electrode System was installed in it. Cyclic voltammetry measurements were run from -0.9 to 1.5 V.

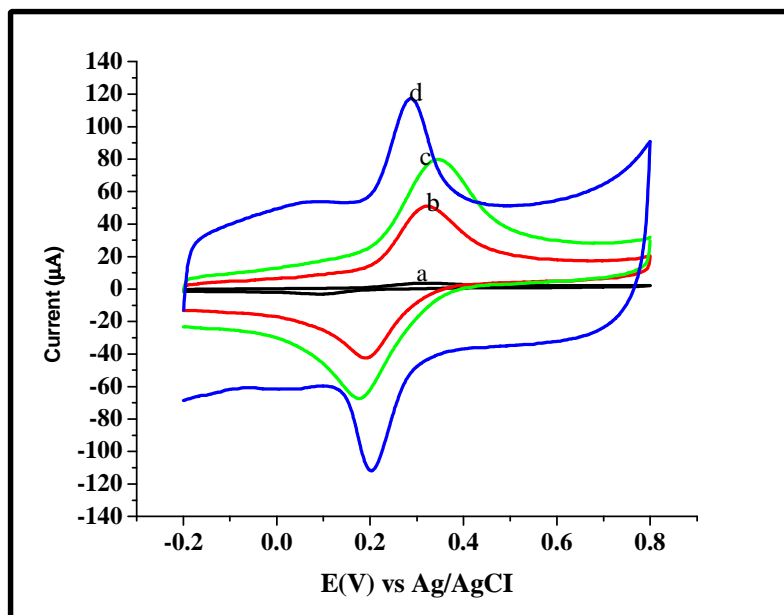


Figure 16. Voltammograms of 100  $\mu\text{M}$  catechol at different electrodes (a) bare GCE (b) SWCNTs/ GCE (c) PEDOT/GCE and (d) SWCNTs/PEDOT/GCE at scan rate of  $100 \text{ m Vs}^{-1}$  in 0.2 M PBS solution (pH 7.0)

From Figure.16 (a) it can be seen that at the bare electrode, the oxidation and reduction of catechol result in broad waves with the corresponding peak potentials of 0.316 V and 0.089 V. Hence it shows irreversible behaviour with ( $\Delta E_p = 0.227 \text{ V}$ ). However, at the SWCNTs/GCE in (Figure 16 (b)), the reversibility of catechol is slightly improved together with the current signal increase. The oxidation peak potential negatively shifts to 0.371 V and the reduction peak positively shifts to 0.168 V with ( $\Delta E_p = 0.203 \text{ V}$ ). In addition, at the PEDOT modified electrode in (Figure.16 (c)) the reversibility of catechol is improved. The oxidation peak potential negatively shifts to 0.317 V and the reduction peak positively shifts to 0.192 V with ( $\Delta E_p = 0.125 \text{ V}$ ). But the composite modified electrode consisting of SWCNTs/PEDOT at the GCE in (Figure.16(d)) the oxidation peak potential negatively shifts to 0.288 V and the reduction peak positively shifts to 0.199 V with ( $\Delta E_p = 0.89 \text{ V}$ ) where, the reversibility of catechol is significantly improved. Also the result shows that 0.2 M  $\text{K}_3\text{Fe}(\text{CN})_6$  is used as a probe to measure the effective surface area of the SWCNTs/PEDOT/GC modified electrode and bare GCE by cyclic voltammetry at different scan rates.

### 3.3.5. Cyclic voltammetric investigation

The electrochemical oxidation of catechol has been studied using cyclic voltammetry and differential pulse voltammetry. The optimum pH needed to study the electrochemical behaviour of catechol was pH 7 phosphate buffer solution.

## 4. Results and discussion

Electrochemical behaviour of the modified electrode shows the cyclic voltammograms of 100  $\mu\text{M}$  catechol at the glassy carbon electrode in pH 7.0 phosphate buffer. The cyclic voltammograms of catechol shows reversible oxidation and reduction peaks. The electrochemical reaction of catechol at SWCNTs/PEDOT/GC modified electrode at pH 7.0 showed an oxidation peak at 0.288 V and a reduction peak at 0.203 V. The separation of peak potentials was about 0.085 V.

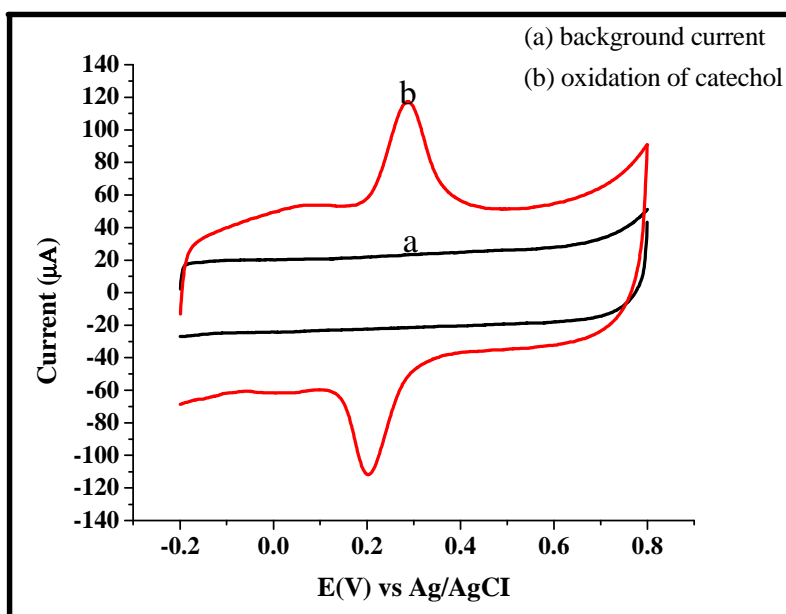


Figure 17. Cyclic voltammograms of 100  $\mu\text{M}$  catechol in 0.2 M  $\text{KH}_2\text{PO}_4\text{-K}_2\text{HPO}_4$  Buffer (pH = 7.0) SWCNT/PEDOT/ GCE with scan rate of 100 mV /s

#### 4.1. Effect of scan rate

On the oxidative current of 100  $\mu\text{M}$  catechol at a SWCNTs/PEDOT/GC modified electrode in 0.2 M  $\text{KH}_2\text{PO}_4$  electrolyte solution was studied. Figure 18 shows the cyclic voltammograms obtained in the potential range of -2.0 to + 0.8 V. To investigate the diffusion behaviour CVs were recorded for the scan rate from 20 to 500 mV/s and a shift in the anodic peak potentials, and change in the magnitude of anodic peak currents was observed. Hence it was found that the electrode reaction of catechol at the surface of the electrode depends on the scan rates.

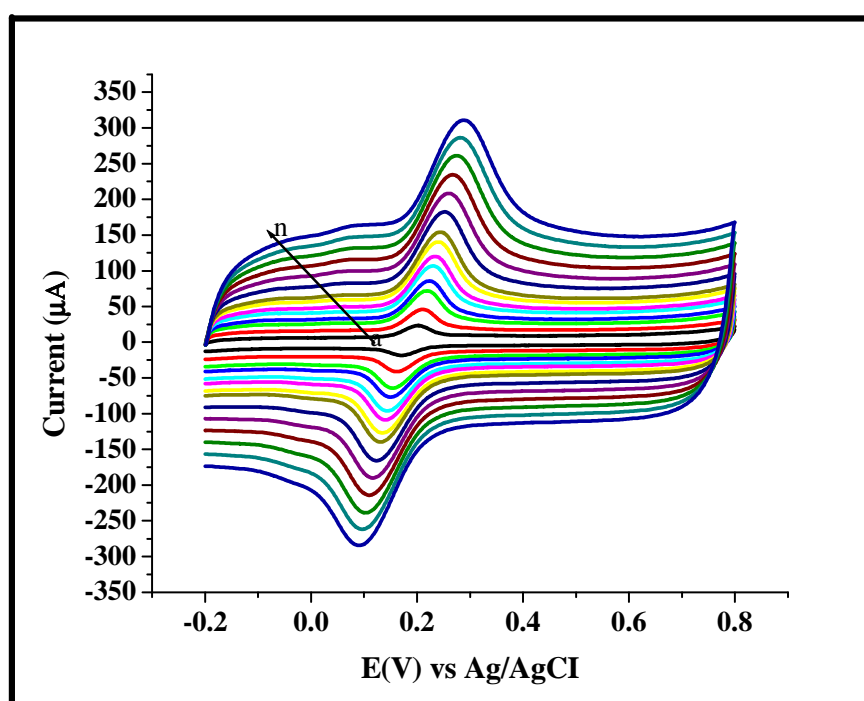


Figure 18. Cyclic voltammograms recorded at SWCNTs/PEDOT/GCE with 100  $\mu\text{M}$  catechol in 0.20 M ( $\text{KH}_2\text{PO}_4$  -  $\text{K}_2\text{HPO}_4$ ) (pH 7.0) at different scan rates: n: 0.02, 0.05, 0.08, 0.10, 0.13, 0.15, 0.18, 0.20, 0.25, 0.30, 0.35, 0.40, 0.45 and 0.5 V/s

In order to investigate the oxidation and reduction behaviour of catechol, the effect of scan rate at the oxidative and reductive peak current of 100  $\mu\text{M}$  catechol at SWCNTs/PEDOT/GC in 0.2M phosphate buffer solution (pH = 7) were investigated. Figure 19 shows both the oxidative and reductive peak current of catechol increased with scan rate (20 to 500 mV/s). Figure.19 also show that the oxidation and the reduction peak current of catechol exhibited a linear relation to the square root of scan rate as ranging from 20 to 500 mV/s. The linear regression equations of the  $I_{pa}$

and  $I_{pc}$  for the scan rates are expressed as  $i_{pa} (A) = 18.7517 - 7.26288v^{1/2}$ ,  $r = 0.998$ ,  $I_{pc}(A) = -30.1626 + 8.47183v^{1/2}$ ,  $r = 0.999$  respectively. The relationship between the oxidation peak current and square root of the scan rate indicates that the oxidation of catechol at the composite modified electrode is a diffusion-controlled process. Scan rate of 100 mV/s was chosen in this work [35].

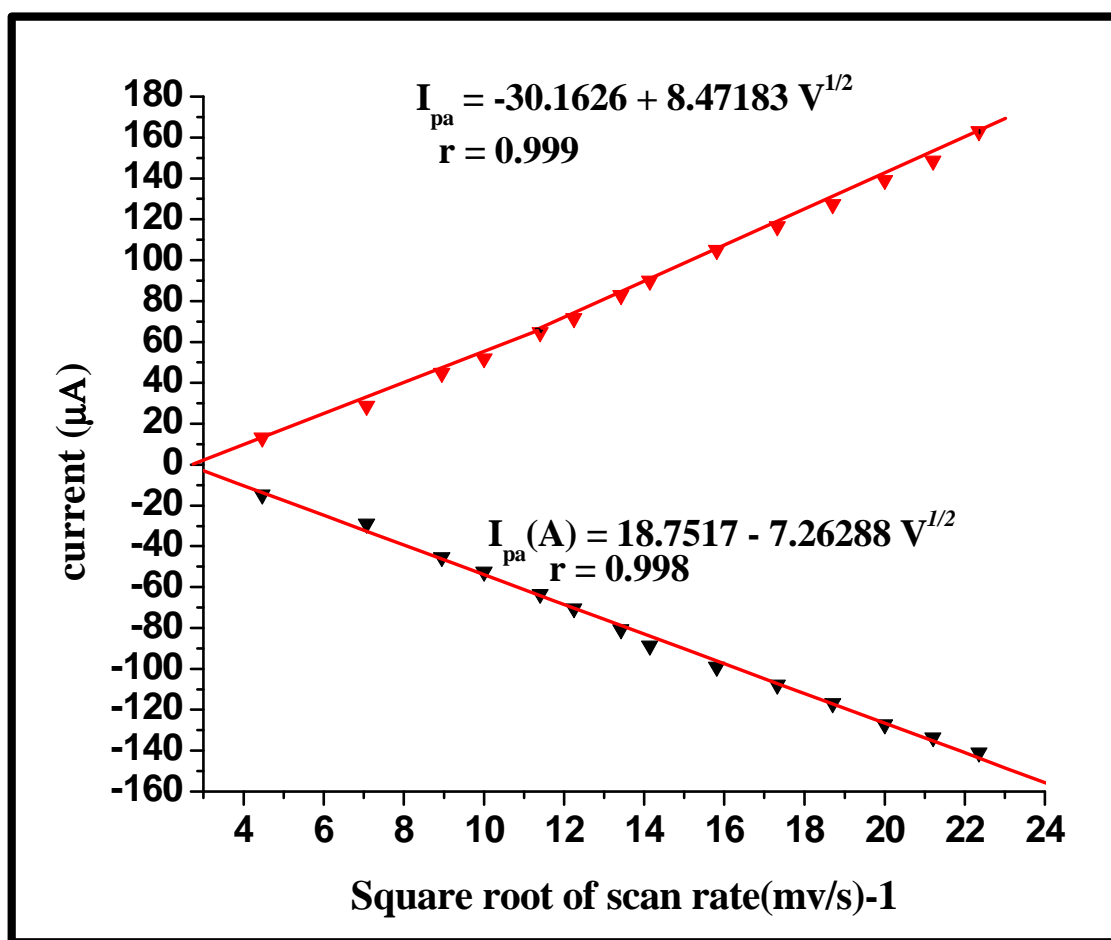


Figure 19. The dependence of the peak current on square root of scan rate

It can be seen that by increasing the scan rate, the anodic and cathodic peak currents increased and both anodic and cathodic peak potentials shifted (Figure 20). The anodic peak potential shifted to more positive potential values, while that of the cathodic peak shifted to more negative values.

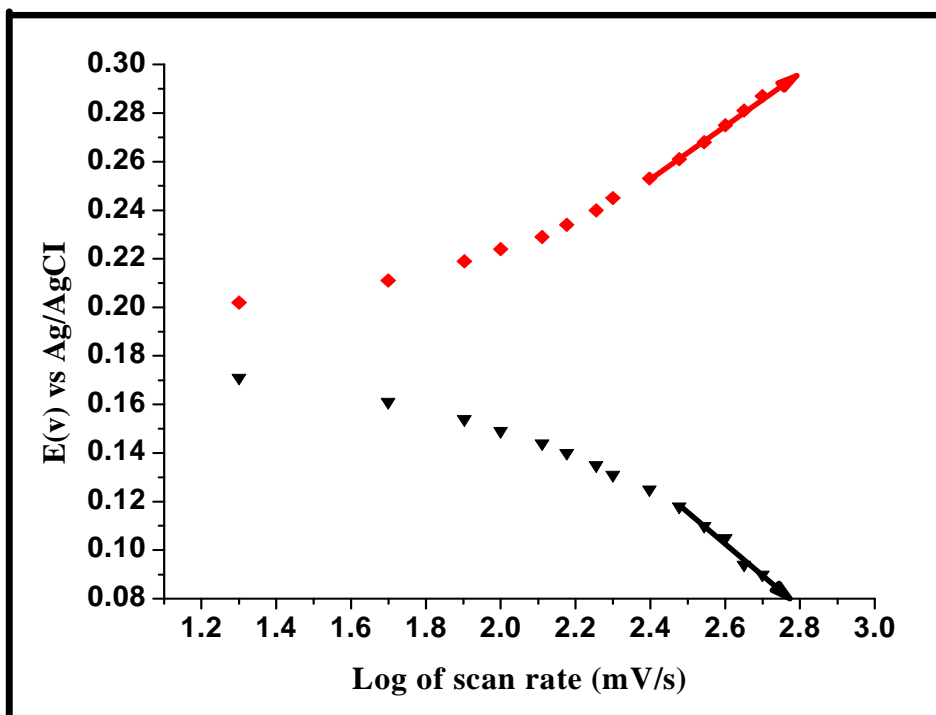


Figure 20. The dependence of the peak potential  $E_p$  on  $\log v$

Table 2. The dependence of the peak current on the square root of the scan rate

scan rate (mVs <sup>-1</sup> )	Square root of scan rate(mVs <sup>-1</sup> )	I <sub>pa</sub> (A)	I <sub>pc</sub> (A)	I <sub>pa</sub> /I <sub>pc</sub>
20	4.47	-1.466E-5	1.315E-5	1.115
50	7.071	-2.900E-5	2.871E-5	1.010
80	8.944	-4.530E-5	4.482E-5	1.010
100	10	-5.238E-5	5.190E-5	1.009
130	11.402	-6.334E-5	6.469E-5	0.98
150	12.247	-7.037E-5	7.161E-5	0.983
180	13.416	-8.058E-5	8.292E-5	0.895
200	14.14	-8.858E-5	9.002E-5	0.943
250	15.81	-9.898E-5	1.050E-4	0.922
300	17.32	-1.076E-4	1.166E-4	0.98
350	18.71	-1.168E-4	1.273E-4	0.914
400	20	-1.271E-4	1.391E-4	0.913
450	21.21	-1.335E-4	1.486E-4	0.898
500	22.36	-1.408E-4	1.631E-4	0.863

Table 3. The dependence of peak potentials on the logarithm of scan rate

scan rate (mvs <sup>-1</sup> )	Logof rate(mV/s)	scan	E <sub>pc</sub> (V)	E <sub>pa</sub> (V)	ΔE <sub>p</sub>
20	1.30		0.171	0.202	0.031
50	1.699		0.161	0.211	0.05
80	1.903		0.154	0.219	0.065
100	2		0.149	0.224	0.075
130	2.11		0.144	0.229	0.085
150	2.176		0.140	0.234	0.094
180	2.255		0.135	0.240	0.105
200	2.30		0.131	0.245	0.114
250	2.398		0.125	0.253	0.128
300	2.477		0.118	0.261	0.143
350	2.544		0.110	0.268	0.158
400	2.60		0.105	0.275	0.170
450	2.65		0.094	0.281	0.187
500	2.699		0.90	0.287	0.197

#### 4.2. Effect of ionic strength

The effect of ionic strength for the phosphate buffer on the anodic peak current of 100 μM catechol was studied using 0.05, 0.1, 0.15, 0.2 M phosphate buffer at pH = 7.0. By increasing the ionic strength of the supporting electrolyte, the peak current increased, so 0.2 M phosphate buffer pH = 7.0 was chosen for further studies [36].

### 4.3. Effect of the pH of the supporting electrolyte

The pH of the media used for the purpose of the accumulation has a profound effect on the voltammetric response. It affects the rate, equilibrium state and the electrode reaction. For that reason this parameter was studied for DPV determination of catechol at the SWCNTs/PEDOT/GC modified electrode in the pH range 4 to 9.

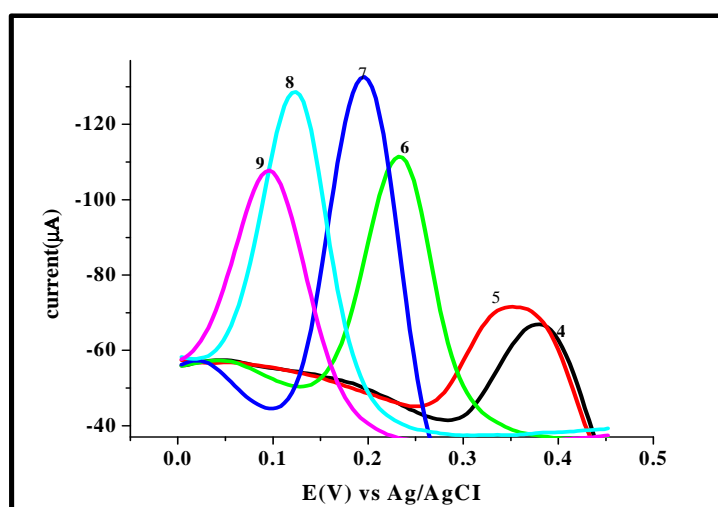


Figure 21. Effect of the pH on DPV response of the modified GC electrode for 100  $\mu\text{M}$  catechol; 0.2 M in phosphate buffer solution

The catechol peak current as a function of pH is shown in Figure 22. Catechol show different voltammetric behaviour in the pH range studied, this may be due to the influence of pH on the accumulation potential. Generally at the modified glassy carbon the amount of accumulated catechol is larger at pH 7.0. According to the observed result at SWCNTs/ PEDOT/GC modified electrode pH = 7.0 was selected to for the determination [37].

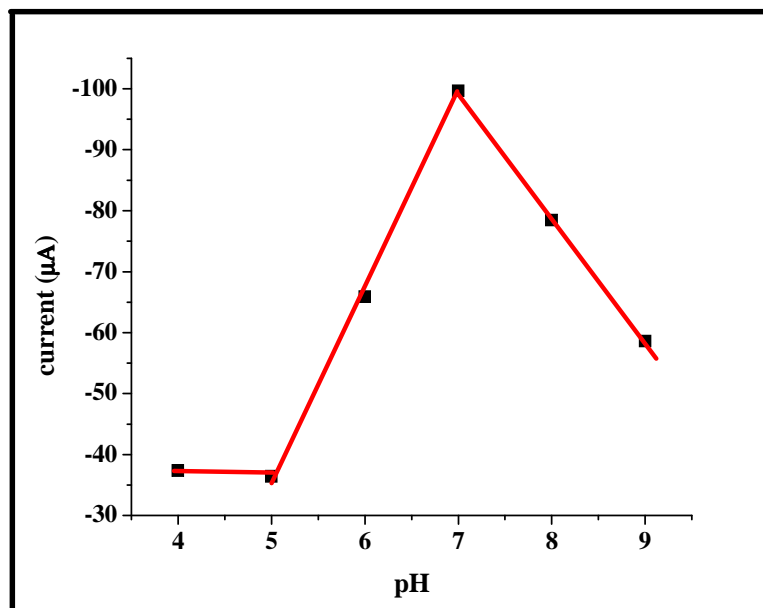


Figure 22. Plot of DPV anodic peak current as a function of pH of 100  $\mu\text{M}$  catechol

Effect of solution pH on the electrochemical signal was analyzed. Figure 23 showed influence of pH on the redox reaction of catechol at SWCNTs/PEDOT/GC modified electrode. The relationship between oxidation potential ( $E_{pa}$ ) and pH can be described using the following equation:  $E_a = 0.63374 - 0.06211\text{pH}$ ,  $r = 0.995$ . Which the slope was 0.062 V, this value is close to the theoretical value of 0.059 V/pH indicating the participation of the same number of electrons and protons in the electrochemical process. The ratio of the number of the electron and proton involved in the reactions is near 1 : 1 ratio. As catechol oxidation is a two-electron process, the number of protons involved is also predicted to be two. Therefore, a mechanism for the catechol oxidation can be proposed as shown in Figure 24.

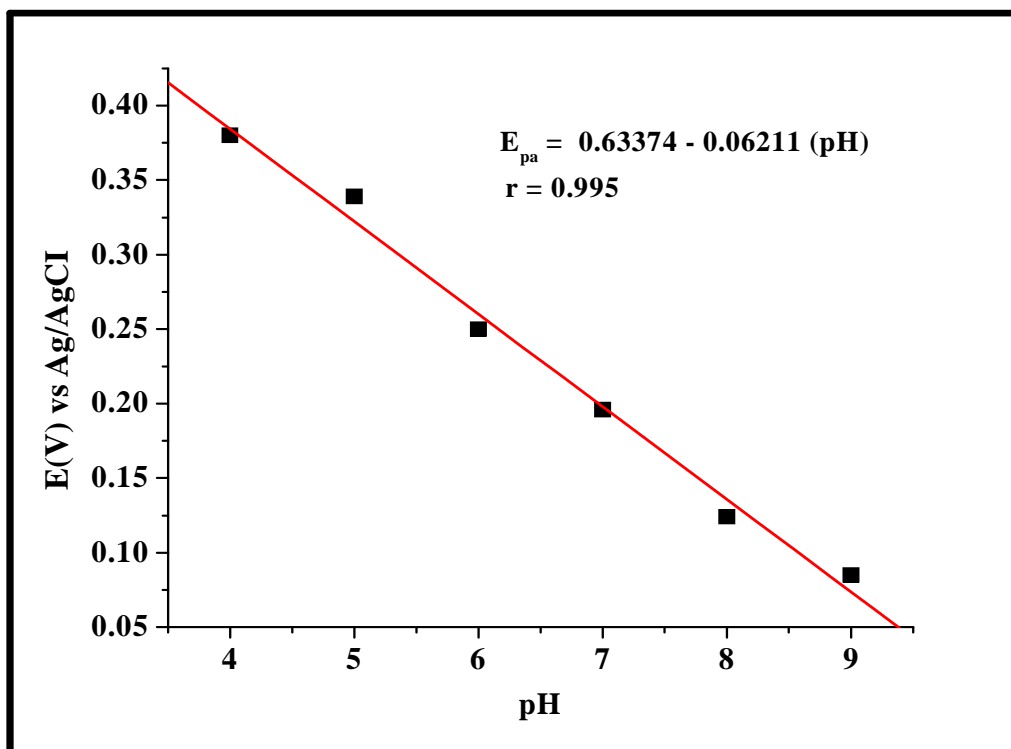


Figure 23. Plot of DPV anodic peak potential as a function of pH for 100  $\mu$ M catechol

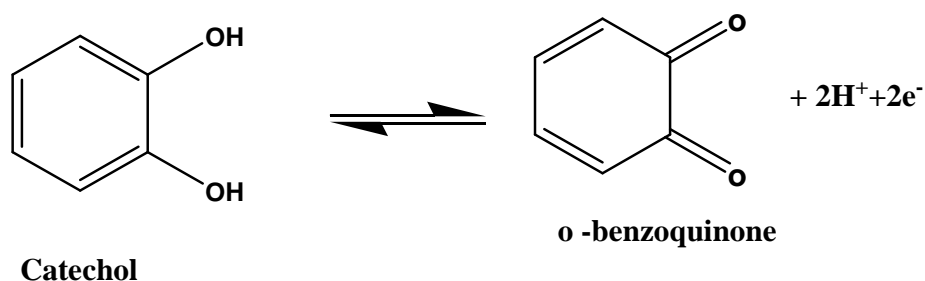


Figure 24. Oxidation of catechol

#### 4.4. Differential pulse voltammetric investigation

The redox peaks obtained for catechol with SWCNTs/PEDOT/GCE modified electrode, the evaluation of the analytical performance of SWCNTs/PEDOT modified GCE for catechol analysis required optimization of many parameters. These include, pulse amplitude, pulse width, pulse period and pH. According to this study, a series of experiment was conducted to attain suitable experimental conditions for the determination of catechol. The effect of particular

variable was studied under identified conditions by keeping all variables constant except one under study.

#### 4.4.1 Effect of pulse amplitude

The effect of the differential pulse amplitude on the current response was studied by varying the differential pulse amplitude from 20 to 100 mV. The result showed that as the amplitude was increased from 20 to 100 mV the peak current also increased. Hence pulse amplitude of 100 mV was chosen for best quantifying catechol for this investigation.

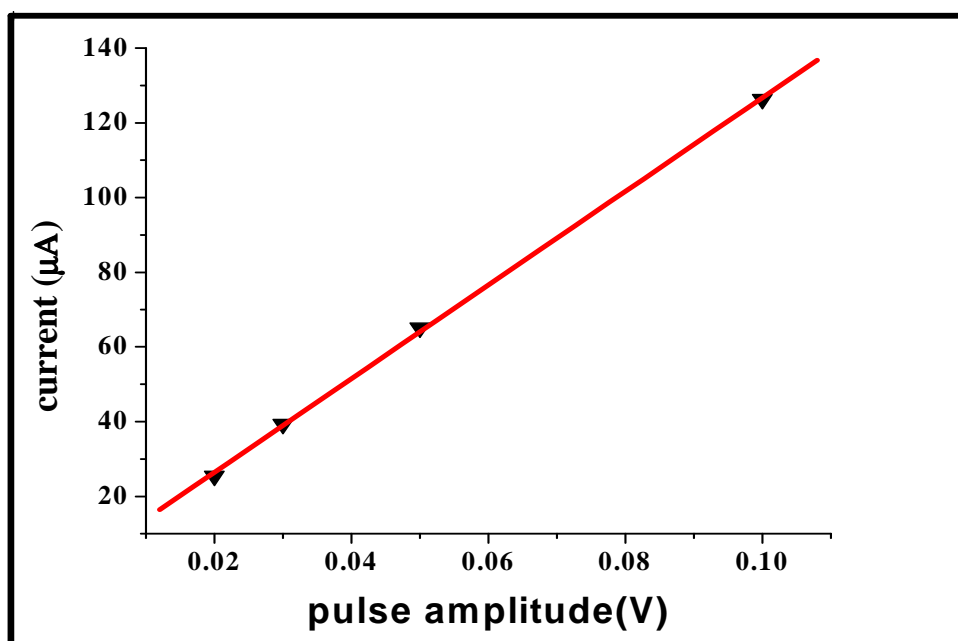


Figure 25. Plot of anodic peak current as a function of differential pulse amplitude

#### 4.4.2. Effect of pulse width

The effect of pulse width on the differential pulse voltammetry peak current of catechol was studied at various pulse widths between 50 ms and 600 ms. The maximum peaks current was obtained at 50 ms as shown in Figure. 26. Therefore the 50 ms was chosen as the optimum pulse width.

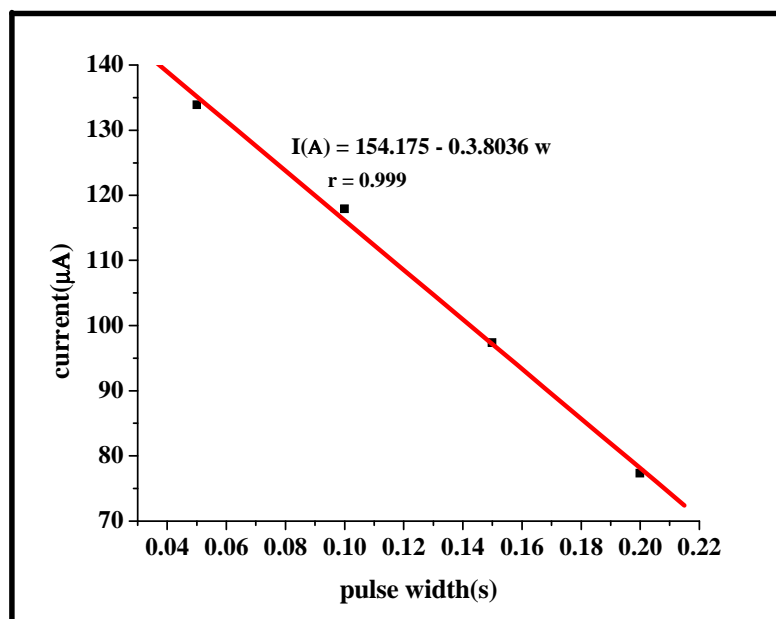


Figure 26. Plot of anodic peak current as a function of differential pulse width

#### 4.4.3. Effect of pulse period

The effect of pulse period on the peak current of catechol was studied using 100 μM catechol. The responses obtained are shown in Figure 27. With the variation of pulse period between 100 to 600 mV the peak current increased with increase in pulse period up to 300 mV and then decreased. So the pulse period of 300 mV was selected as an optimum pulse period for further experiments.

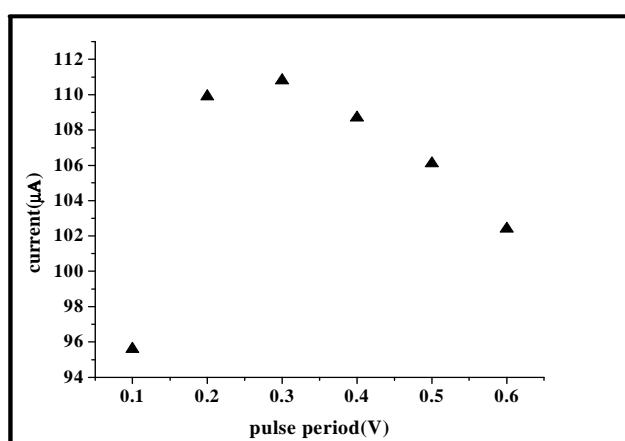


Figure 27. Plot of anodic peak current as a function of differential pulse period

#### 4.4.5. Optimized Experimental Conditions

The effect of pulse amplitude, pulse width and pulse period were studied to obtain the optimized experimental conditions for differential pulse voltammetric determination of catechol at SWCNTs/PEDOT/GC modified electrode. The optimum parameters identified for the determination of the analyte for plotting the calibration curve are summarized as follows.

Table 4. Optimum experimental conditions for the determination of catechol by DPV as SWCNTs/PEDOT/GC modified electrode.

<b>Parameters</b>	<b>Optimum value</b>
<b>Pulse amplitude</b>	0.1 V
<b>Pulse width</b>	0.05 s
<b>Pulse period</b>	0.3 s
<b>pH</b>	7

#### 4.5. Linear Range and Detection Limit

The analytical utility of a given procedure depends on achieving well defined concentration dependence. According to the optimum experimental conditions described above; the dependence of the voltammetric signal on the concentration of catechol and the sensitivity of the method are illustrated by differential pulse voltammetry for different concentration of catechol( Figure 28). Figure 28 shows some of the typical DPV voltammograms recorded on the SWCNTs/PEDOT/GC modified electrode for different catechol concentrations.

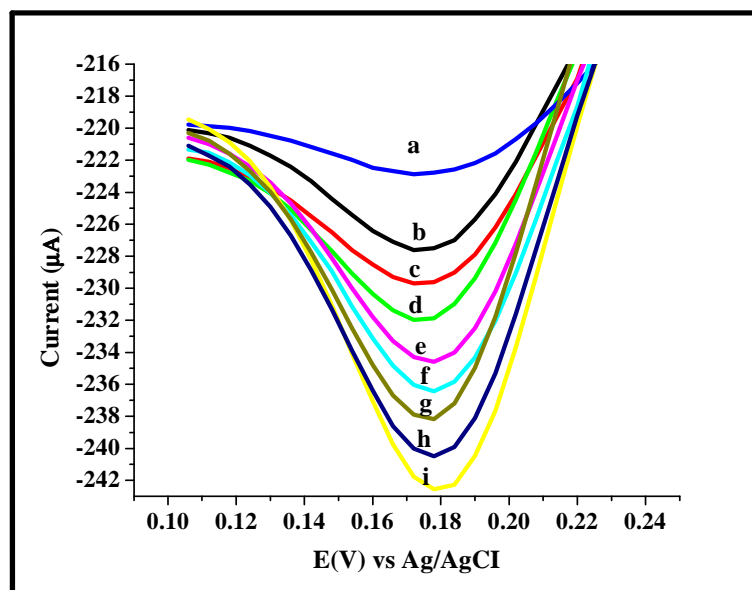


Figure 28. Differential pulse voltammograms for SWCNTs/PEDOT/GC modified electrode for different concentration of catechol. Pulse amplitude 100 mV, pulse width 50 ms and pulse period 300 mV

Table 5. Comparison of characteristics obtained from some literatures and this work

Sensor	Linear range( $\mu\text{M}$ )	LOD( $\mu\text{M}$ )	Reference
<b>p-Phe/GCE</b>	10–140	0.7	[38]
<b>Penicillamine/GCE</b>	25–175	0.6	[39]
<b>Tyr/GCE</b>	60–800	6	[40]
<b>MWCNT/GCE</b>	20–1200	10	[41]
<b>(CILE/GCE</b>	1-800	0.6	[42]
<b>SWCNTs/PE DOT/GCE</b>	6-100	0.18	This work

The peak height for catechol was found to increase with increase concentration from 6 to 100  $\mu\text{M}$ . The calibration curves for 9 data points was found to be linear with  $r = 0.998$  with regression equation of  $Y = A + B \cdot C$  Where  $A = -18.643$  and  $B = -0.172555$ . As it is indicated using the numerical value of regression coefficient,  $r$  for this experiment, the data sets showed a good linear fit because the value of  $r$  is close to one. The detection limit for catechol, considering signal-to-noise ratio of three was found to be  $1.8 \times 10^{-7} \text{ molL}^{-1}$ . Figure 29 shows a calibration curve for differential pulse voltammograms at SWCNTs/PEDOT/GC modified electrode for the catechol concentration range 6 -100  $\mu\text{M}$ .

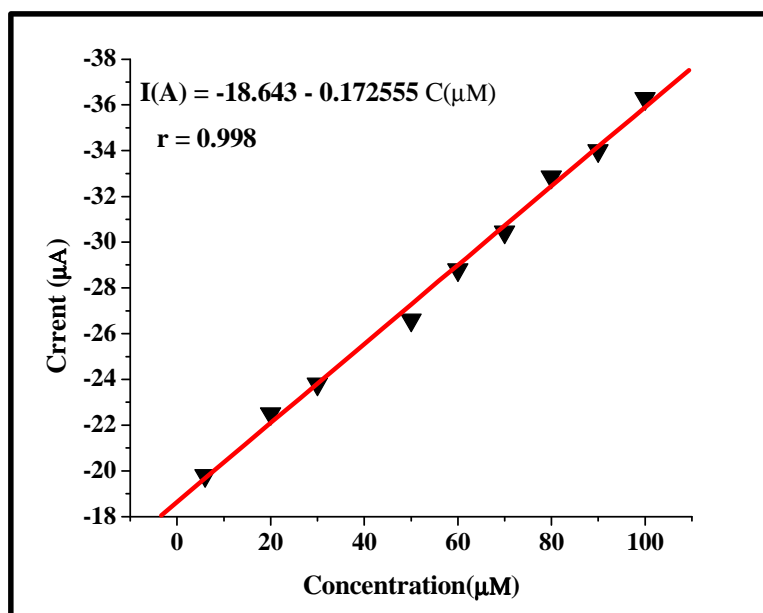


Figure 29. Plot of DPV anodic peak current as a function of catechol concentration from 6 to 100  $\mu\text{M}$

#### 4.6. Effect of Interferences

Possible interferences in the detection of catechol such as ascorbic acid, uric acid and hydroquinone at SWCNTs/PEDOT/GC modified electrode were studied. 20  $\mu\text{M}$  catechol was added to 20, 40, 100, 200 and 2000  $\mu\text{M}$  of the above interferon and differential pulse voltammogram was recorded between 0.01 V and 0.55 V. The effect of ascorbic acid, as one of the most interfering substances in the electrochemical determination of some organic compounds was examined. Figure 30 shows the effects of different concentrations of ascorbic acid on the peak height of 20  $\mu\text{M}$  catechol. As result the addition of ascorbic acid has no marked effect (peak current change below 5%) on addition of 2, 5, 10 and 100-fold ascorbic acid on the response of catechol. So that catechol can be detected in the presence of ascorbic acid [43].

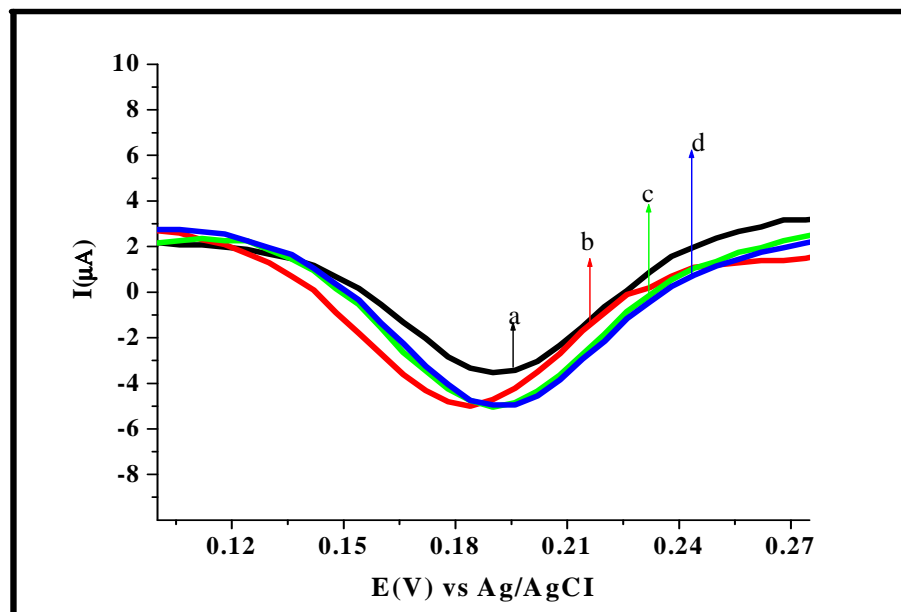


Figure 30. Differential pulse voltammograms for SWCNTs/PEDOT/GC modified electrode for, (a) 40, (b) 100, (c) 200 and (d) 2000  $\mu\text{M}$  ascorbic acid. Amplitude 100 mV, pulse width 50 ms and pulse period 300 mV

Interference studies were performed using DPV at SWCNTs/PEDOT/GC modified electrode in the presence of different concentrations of hydroquinone while the concentration of catechol was kept constant. (Figure.31).the peak currents for hydroquinone showed a linear increase in the range of 20–2000  $\mu\text{M}$ . From Figure 31 it could be seen that increase in hydroquinone concentration did not affect the response current of catechol. The peak current for catechol remained constant and overlapping peaks of catechol with no shift were observed. Also as it can be seen from Figure.31 the influences of hydroquinone was negligible (signal change below 5%) as a result determination of catechol in the presence of hydroquinone is possible because their oxidation potentials are different and the peaks for catechol and hydroquinone are very well resolved [44].

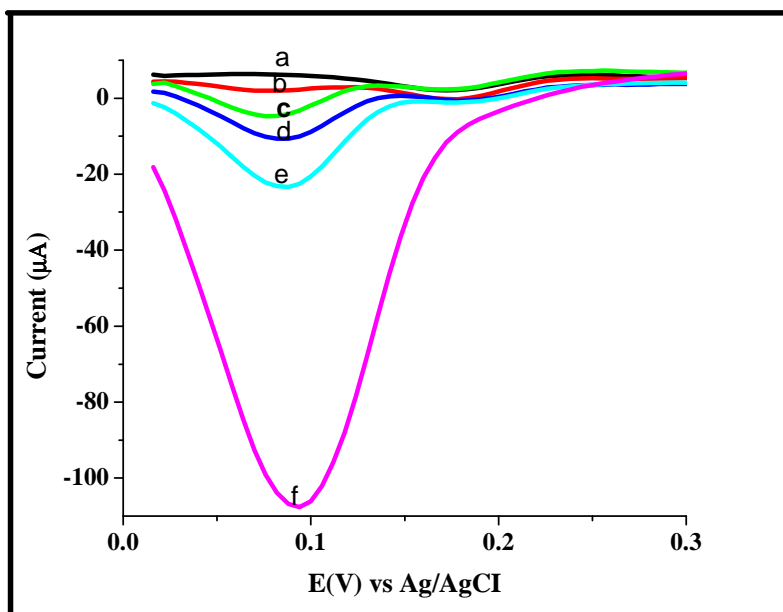


Figure 31. Differential pulse voltammograms at SWCNTs/PEDOT/GC modified electrode for (a) 0, (b) 20, (c) 40, (d) 100, (e) 200 and (f) 2000  $\mu\text{M}$  hydroquinone. Amplitude 100 mV, pulse width 50 ms and pulse period 300 mV

It was also observed that the oxidation peak potential of uric acid was much more positive than catechol. The oxidation of uric acid at the modified electrode occurs at  $-0.405\text{ V}$  (Figure 32), with no possible interference on the detection of catechol. This was confirmed as the oxidation currents of catechol were not affected in the presence of 1, 2, 5, 10 and 100-fold uric acid [45].

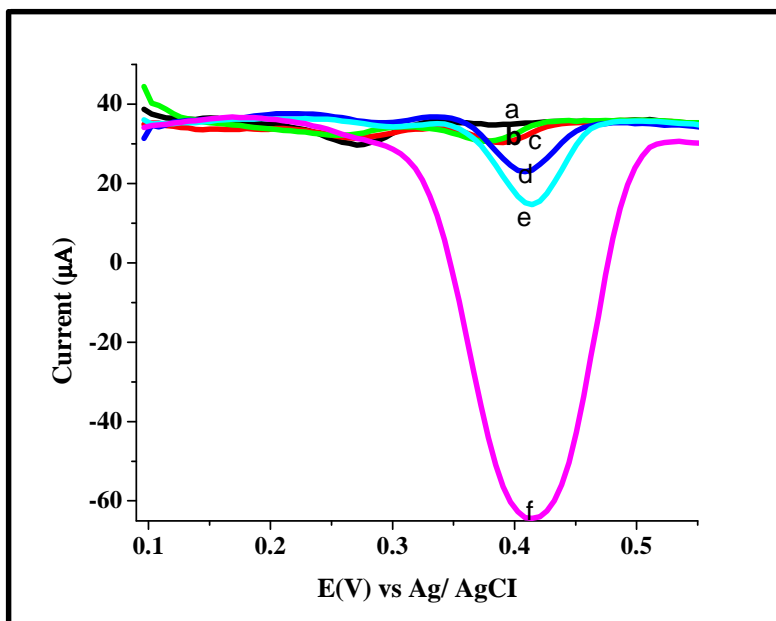


Figure 32. Differential pulse voltammograms for SWCNTs/PEDOT/GC modified electrode for different concentration of uric acid which is (a) 0, (b) 20, (c) 40, (d) 100, (e) 200 and (f) 2000  $\mu\text{M}$ . Amplitude 100 mV, pulse width 50 ms and pulse period 300 mV

#### 4.7. Simultaneous determination of hydroquinone and catechol

The results in Figure 31 indicate that the SWCNTs/PEDOT/GC modified electrode showed an excellent response for the oxidation of hydroquinone and catechol. In DPV measurements, the oxidation potential of hydroquinone at the SWCNTs/PEDOT/GC modified electrode was found to be more negative potential than that of catechol. Therefore, this fact encouraged us to apply the SWCNTs/PEDOT/GC modified electrode for the simultaneous determination of hydroquinone and catechol.

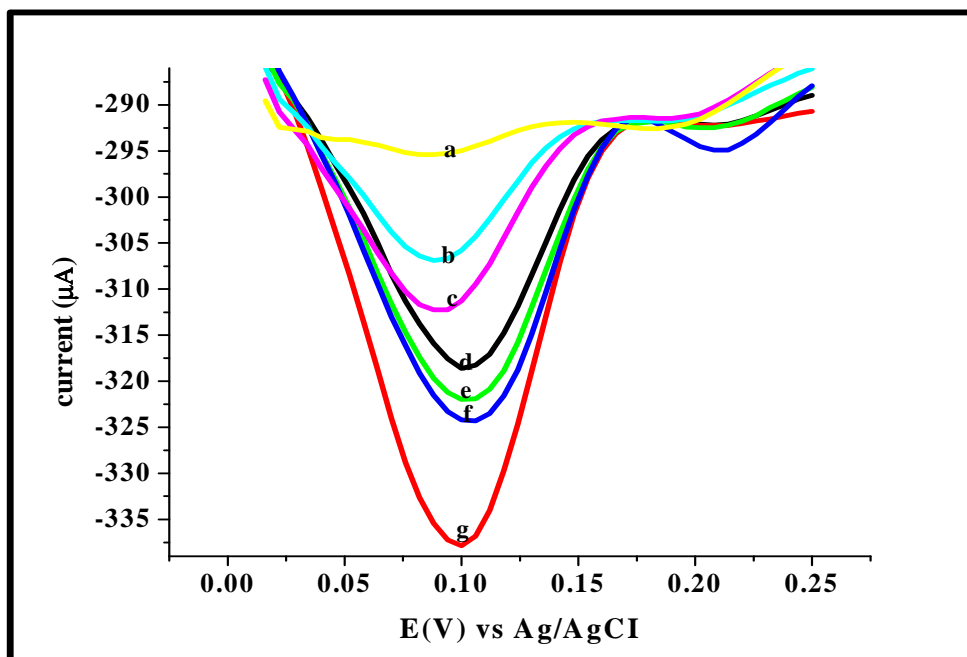


Figure 33. DPV for the binary mixtures of hydroquinone and catechol at SWCNTs/PEDOT/GC modified electrode in 0.2 M PBS (pH 7.0), [catechol] was kept constant and [hydroquinone] was changed (i.e., [catechol] = 20  $\mu\text{M}$ , [catechol]: (a) 20, (b) 40, (c) 60, (d) 70, (e) 80, (f) 100, (g) 150  $\mu\text{M}$ )

Thus attempt was made to determine hydroquinone and catechol simultaneously by using the composite modified electrode with DPV. Figure.33 above shows the DPV at different concentration of hydroquinone while the concentration of catechol was kept constant. As shown in Figure.34 the oxidation peak current for hydroquinone increased linearly with increasing hydroquinone concentration in the range of 20 – 700  $\mu\text{M}$ . The linear regression equation was  $i_{pa}(\mu\text{A}) = -10.9207 - 2.84952 C (\mu\text{M})$  with correlation coefficient ( $r$ ) = 0.995. Furthermore, the peak current for hydroquinone increased with increase in hydroquinone concentration, the peak current of catechol remained almost constant. Thus, it is confirmed that the responses of hydroquinone and catechol at the composite modified electrode are independent.

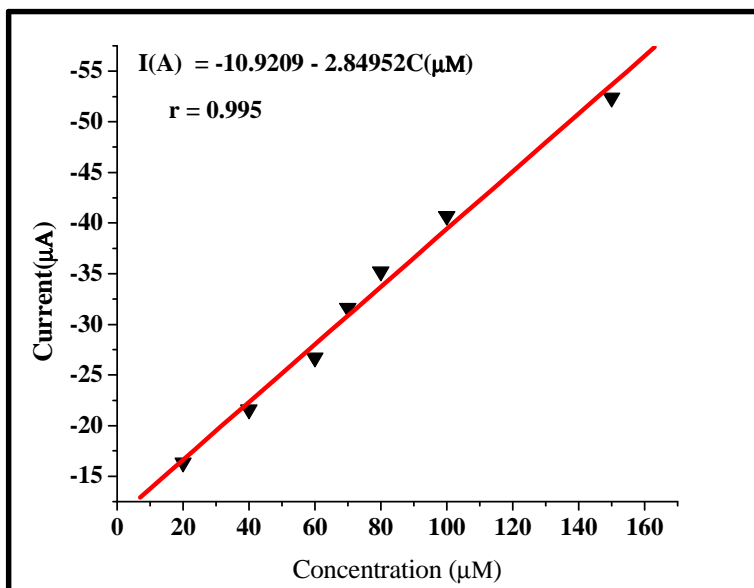


Figure 34. Calibration plot of hydroquinone in the presence of 20 μM catechol

Figure.35 shows the DPV curves for different concentrations of catechol while the concentration of hydroquinone was kept constant. Here also the oxidation peak current for catechol increased linearly with increase in the concentration catechol in the range of 20 μM – 150 μM as shown in Figure 35 below.

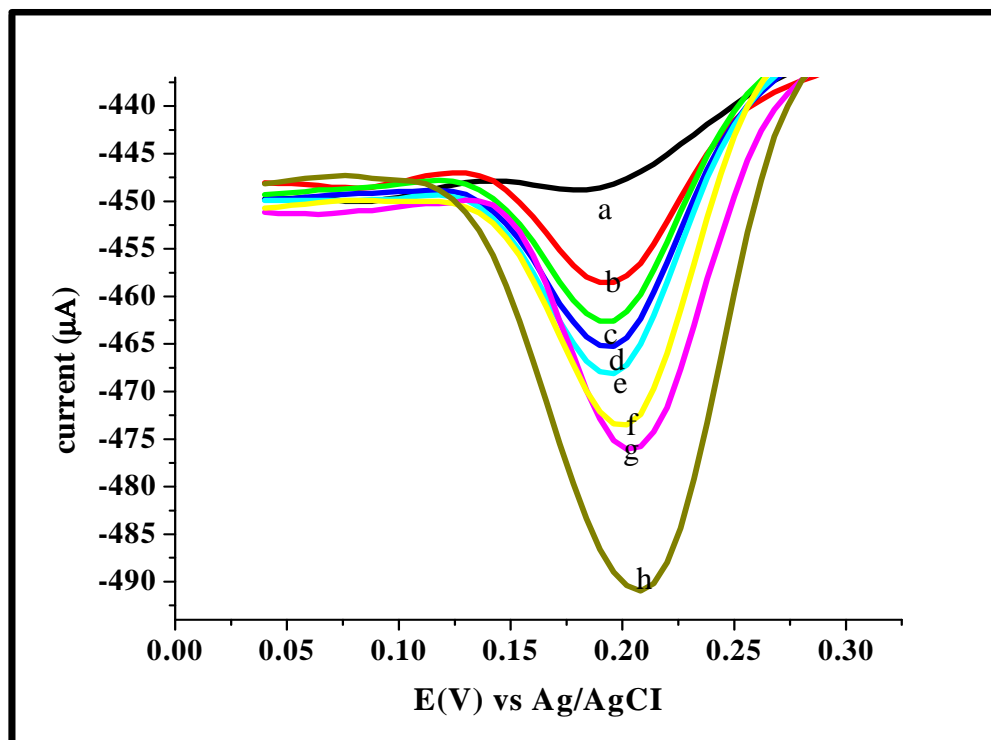


Figure 35. DPVs for the binary mixtures of hydroquinone and catechol at SWCNTs/PEDOT/GC modified electrode in 0.2 M PBS (pH 7), [hydroquinone] was kept constant and [catechol] was changed (i.e., [hydroquinone] = 20  $\mu\text{M}$ , [catechol]: (a) 20, (b) 40, (c) 60, (d) 70, (e) 80, (f) 100, (g) 150  $\mu\text{M}$ ).

The linear regression equation found was  $i_{pa}/A = -5.35223 - 0.338256 C(\mu\text{M})$  with correlation coefficient ( $r$ ) = 0.999. Furthermore, the peak current for catechol increased with the increase in the concentration of catechol, the peak current for hydroquinone remained almost constant. This suggests that fouling due to the oxidized product of hydroquinone affecting the response for catechol does not occur at the composite modified electrode. Thus, the simultaneous selective and sensitive determination of hydroquinone and catechol was achieved at the SWCNTs/PEDOT/GC modified electrode.

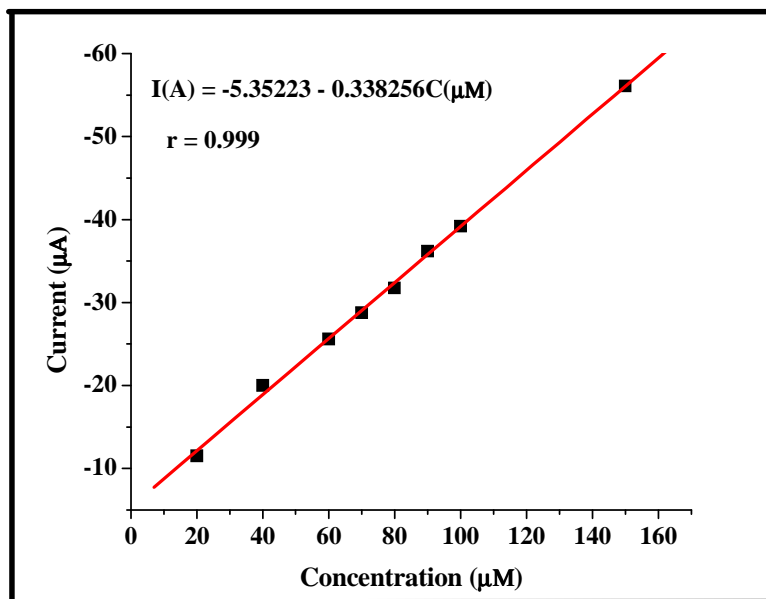


Figure 36. Calibration plot of catechol in the presence of 20 μM hydroquinone

## 4.8 Analytical applications

### 4.8.1 Analysis of Catechol in tap water

The analytical utility of the method was evaluated by applying it to the determination of catechol in the tap water using differential pulse voltammetry at the SWCNTs/PEDOT/GCE for 0.2 molL<sup>-1</sup> PBS (pH 7.0). In order to test the validity of the method, the proposed procedure was applied for determination of catechol in tap water sample by adding a known amount of catechol to the tap water. 4, 5, 6 and 7 μM were spiked into the known amount of catechol and differential pulse voltammograms were recorded at optimum conditions for each addition then the peak current reading were used to calculate the concentration. The result demonstrated that it is possible to determine the concentration of catechol in real water sample solutions. The results are summarized in Table 6.

Table 6. Recovery Study

<b>Sample No.</b>	<b>Original[CC](<math>\mu\text{M}</math>)</b>	<b>CC added(<math>\mu\text{M}</math>)</b>	<b>CC found(<math>\mu\text{M}</math>)</b>	<b>Recovery (%)</b>
<b>1</b>	<b>2.0</b>	<b>4</b>	<b>6.004</b>	<b>100.1</b>
<b>2</b>	<b>2.0</b>	<b>5</b>	<b>6.920</b>	<b>98.40</b>
<b>3</b>	<b>2.0</b>	<b>6</b>	<b>8.001</b>	<b>100.01</b>
<b>4</b>	<b>2.0</b>	<b>7</b>	<b>8.978</b>	<b>99.69</b>

From Table 6 it can be seen that the results were satisfactory with recovery in the range of 98.40–100.1% for catechol. So the proposed electrode could be efficiently used for the determination of catechol content in water samples with satisfactory results.

#### **4.8.2. Analysis of catechol in tea samples**

For the detection of catechol in tea samples a known amount (15.0 g) was weighed and dissolved in 250 ml of double distilled water followed by boiling for 1 h on a hot plate with stirring. After allowing the residue to settle, the hot solution was filtered and then used for further experiments. A known amount (1 ml) of this solution was added to 100 ml electrolyte solution of pH = 7.0. First the DPV of the diluted tea solution was run and then 2, 4, 6 and 8  $\mu\text{M}$  of catechol were added in to the tea sample to estimate the presence of catechol. The quantitative determination of catechol was done by using calibration curve using differential pulse voltammetry (DPV). To

further verify the applicability of the proposed modified GCE for the determination of catechol, the method was used for the quantitative analysis of local tea. With unknown amount of catechol in tea samples, recovery experiments were performed by measuring the current responses of the samples in which known concentration of catechol were added. The amount of catechol in the tea samples was calculated based on the calibration curve and it was found to be 0.15  $\mu\text{M}$ . The obtained results are given in Table 7. The recovery ranged from 99.66 to 105.25% which is very good. Thus the applicability of the SWCNTs/PEDOT/GCE modified electrode and differential pulse voltammetry was effective for the determination of catechol.

**Table 7. Recovery Study**

Sample No.	added CC( $\mu\text{M}$ )	Found CC( $\mu\text{M}$ )	Recovery (%)
1	2.0	2.046	102.23
2	4.0	3.987	99.68
3	6.0	6.315	105.25
4	8.0	7.973	99.66

## **5. Conclusion**

A composite of SWCNTs and conducting polymers (PEDOT) were electrode posited onto the surface of glassy carbon electrodes by voltammetry from aqueous solution. The electrocatalytic properties of the resulting polymer films were examined in H<sub>2</sub>SO<sub>4</sub> and in phosphate buffer solutions. The composite of SWCNTs with conducting polymers (PEDOT) showed excellent electrocatalytic property for the oxidization of catechol by significantly lowering the catechol oxidization potential and accelerate the electron transfer rate of the redox reaction. Differential pulse voltammetric parameters and pH were optimized to study their effects on the peak current and the peak potential. Reversible reaction with the transfer of two electrons per molecule of catechol was observed. The modified electrode showed a good sensitivity and selectivity with a very good detection limit and acceptable recovery.

## 6. References

- [1]. J-T. Han, K-J. Huang, J. Li, Y-M. Liu and M. Yu,  $\beta$ - cyclodextrin-cobalt ferrite nanocomposite as enhanced sensing platform for catechol determination, *Colloids and Surfaces B: Biointerfaces*, 98 (58– 62) 2012.
- [2]. L. Ma and G. Zhao, simultaneous determination of hydroquinone, catechol and resorcinol at graphene doped carbon ionic liquid electrode *international journal of electrochemistry*, 6 (1-8)2012.
- [3]. J. Varagnat, Hydroquinone, resorcinol, and catechol. *Kirk-Othmer Encycl. Chem. Technol*, 3rd Ed, 13(39-69) 1984.
- [4]. S. Suresh, V.C. Srivastava and I.M. Mishra, Adsorbtion of catechol, resorcinol, hydroquinone and their derivatives, *International Journal of Energy and Environmental Engineering*, 3(32)2012.
- [5]. P. Gerike and W. K. Fischer, robust summaries of reliable studies for pyridine and pyridine derivatives HPV category, *Ecotoxicology and environmental safety*, 3(159-173)2003
- [6]. D. Manohan and W. Wai, Characterization of Polyphenol Oxidase Sweet Potato (*Ipomoea Batatas* (L.)), *journal for the advancement of science & arts*, 3(14 – 31 ) 2012.
- [7]. K. Verschueren, *Handbook of Environmental Data on Organic Chemicals*, 3rd Ed., New York, Van No strand Reinhold, 5(429–431) (1996).
- [8]. N. Schweigert, A.J.B. Zehnder and R.I.L. Eggen, Chemical properties of catechols and their molecular modes of toxic action in cells from microorganisms to mammals, *Environmental Microbiology*, 3(81-91)2001.
- [9]. D.Rajkumar, J.Kim and K.K.Kim, A study one electrochemical oxidation of catechol in chloride medium for wastewater treatment application, *Environmental engineering*, 9(279-287)2004.
- [10]. A, Kumar, S, Kumar and S. Kumar, adsorption of resorcinol and catechol on Activated carbon: equilibrium and kinetics, 41(3015–3025) 2003.

- [11]. Y.Liao, X. Zhou, J. Yu, Y. Cao, X. Li, and B. Kuai, The Key Role of Chlorocatechol 1,2-Dioxygenase in Phytoremoval and Degradation of Catechol by Transgenic Arabidopsis Physiology, 2(142)2006.
- [12]. W. Liu, L. Wu, X. Zhang and J. Chen, Highly-selective electrochemical determination of catechol based on 3-aminophenylboronic acid-3,4,9,10-perylene tetra carboxylic acid functionalized carbon nanotubes modified electrode, analytical method, 6(718–72) 2014.
- [13]. J. Michałowicz and W. Duda, Phenols Sources and Toxicity, Polish Journal of Environmental. Studies, 16(347-362)2007.
- [14]. T. Tanaka, Y. Matsuo, and I. Kouno, chemistry of secondary Polyphenols produced during processing of tea and selected foods, molecular sciences, 11(14–40)2010.
- [15]. J. Wang, G. Cai, X. Zhu and X. Zhou, Oxidative Chemical Polymerization of 3, 4-Ethylenedioxythiophene and Its Applications in Antistatic Coatings, Journal of Applied Polymer Science, 1(109-115)2011.
- [16]. M. A. Rahman, P. Kumar, D-S. Park and Y-B. Shim, Electrochemical Sensors Based on Organic Conjugated Polymers, Sensors, 8(118-141) 2008.
- [17]. A. Elschner, S. Kichmeyer, W. Iovenich, U. Merker and K. Reuter, principles and application of an intrinsically conductive polymer 2011.
- [18]. M.G. Han and S.H. Foulger 1 Dimensional structures of poly (3,4-ethylenedioxythiophene) (PEDOT): a chemical route to tubes, rods, thimbles, and belt, Chemical Communications, 8(3092–3094)2005.
- [19]. L.B. Groenendaal, F. Jonas, D. Freitag, H. Pielartzik and R. Reynolds, poly (3,4-ethylenedioxythiophene) and derivatives: past, present and future advanced material, 12(1 – 13)2000.
- [20]. A. Arias-Pardilla, T.F. Otero, R. Blancob and J.L. Segura, Synthesis, electropolymerisation and oxidation kinetics of an anthraquinone functionalized poly (3,4-ethylenedioxythiophene), Electrochemical Acta, 55(1535–1542) 2010.

- [21]. A. Elschner, S. Kichmeyer, W. Iovenich, U. Merker and K. Reuter, principles and application of an intrinsically conductive polymer 2011.
- [22]. T.A. Skotheim and J.R. Reynolds conjugated polymers: theory; synthesis, properties, and characterization, 3rd edition, 2007.
- [23]. M.C. Yan, D-E. Tallman, S.C. Rasmussen and G.P. Bierwagena, Corrosion Control Coatings for Aluminium Alloys Based on Neutral and n-Doped Conjugated Polymers, Electrochemical society, 156 (360-366)2009.
- [24]. W. Shenggao, W. Tao, L. Yanqiong, Z. Xiujian, H. Jianjun and W. Jianhua, Plasma Activation of Integrated Carbon Nanotube Electrodes for Electrochemical Detection of Catechol, Plasma Science and Technology, 2(193-197) 2007.
- [25]. <http://www-chem.harvard.edu/htm>.
- [26]. [http://www.rpi.edu/dept/phys/SCIT/Future technologies/nanotubes.html](http://www.rpi.edu/dept/phys/SCIT/Future%20technologies/nanotubes.html).
- [27]. <http://www.azonano.com/>.
- [28]. <http://www.en.wikipedia.org/wiki/nanomaterial>.
- [29]. J.A. Bard and L. R. Faulkner, Electrochemical Methods: Fundamentals and Applications, Second Edition, (2001).
- [30]. P.T. Kissinger and W.R. Helneman, Cyclic voltammetry, Journal of chemical education, 60(702-706)1983.
- [31]. A.I. Remes, multi-wall carbon nanotubes based composite electrodes for Electroanalysis applications, Timișoara, January 2012
- [32]. K. David and J. Gosser, Cyclic Voltammetry: Simulation and Analysis of Reaction Mechanisms, VCH Publishers (1993).
- [33]. D. A. Skoog, D. M. West and, F. J. Holler, Fundamentals of Analytical chemistry, 7th Edition, Harcourt, 1996.

- [34]. W. Liu, L. Wu, X. Zhang and J. Chen, Highly-selective electrochemical determination of catechol based on 3-aminophenylboronic acid-3,4,9,10-perylene-tetracarboxylic acid functionalized carbon nanotubes modified electrode, *Anal. Methods*, **6**(718-724) 2014.
- [35]. M. Chen, X. Li, and X. Ma, Selective Determination of Catechol in Wastewater at Silver Doped Polyglycine Modified Film Electrode, *International Journal Electrochemical Science*, **7** (2616–2622) 2012.
- [36]. L.M. Fotouhi, M, M, M.M. Khakpour, D. Nematollahi, and M.M. Heravi, Investigation of the electrochemical behaviour of some catechols the presence of 4, 6-dimethylpyrimidine-2-thiol, *ARKIVOC*, **2** (43-52) 2008.
- [37.] M. Wei, W. Liu, Z-Z. Gu and Z-D. Liu, electrochemical detection of catechol on boron-doped diamond electrode modified with au/tio<sub>2</sub> Nanorod composite, *journal of the chinese chemical society*, **58**(516-521) 2011.
- [38]. L. Wang<sup>1</sup>, P. Huang, J. Bai, H. Wang<sup>1</sup>, L. Zhang and Y. Zhao, Simultaneous Electrochemical Determination of Phenol Isomers in Binary Mixtures at a Poly(phenylalanine) Modified Glassy Carbon Electrode, *Int. J. Electrochem. Sci*, **1**(403-413) 2006
- [39]. L. Wang, P.F. Huang, J.Y. Bai, H.J. Wang, L.Y. Zhang and Y.Q. Zhao, Covalent modification of glassy carbon electrode with aspartic acid for simultaneous determination of hydroquinone and catechol, *Microchim Acta*, **51** (1581) 2007.
- [40]. S. Tembe, S. Inamdar, S. Haram, M. Karve and S.F.D. Souza, electrochemical – material science – Bio sensors – Li-ion battery – energy materials, *J. Biotechnol*, **128** (80 - 85) 2007.
- [41]. Z. Xu, X. Chen, X.H. Qu and S.J. Dong, Carbon Nanotechnology. Recent Developments in Chemistry, Physics, Materials, *Electroanalysis*, **684**(16) 2004.
- [42]. W. Sun, Y. Li, M. Yang, J. Li and K. Jiao, Application of carbon ionic liquid electrode for the electrooxidative determination of catechol, *Sensors and Actuators B*, **133** (387–392) 2008.

[43]. Y. Kong, Y. Xu, H. Mao, C. Yao and X. Ding, Expanded graphite modified with intercalated montmorillonite for the electrochemical determination of catechol, *Electroanalytical Chemistry*, 669 (1–5) 2012.

[44]. Jin-T. Han, K-J. Huang, J. Li, Y-M. Liu and M. Yu,  $\beta$ -cyclodextrin-cobalt ferrite nanocomposite as enhanced sensing platform for catechol determination, *Colloids and Surfaces B: Biointerfaces*, 98(58– 62) (2012).

[45]. T.C. Canevari, L.T. Arenas, R. Landers, R. Custodio and Y. Gushikem, Simultaneous electroanalytical determination of hydroquinone and catechol in the presence of resorcinol at an  $\text{SiO}_2/\text{C}$  electrode spin-coated with a thin film of  $\text{Nb}_2\text{O}_5$ , *Analyst*, 138(315-324) 2013.